

23 DEC 2004

FI 1066234

REC'D 30 SEP 2003

WIPO

PCT

THE UNITED STATES OF AMERICA

TO ALL TO WHOM THESE PRESENTS SHALL COME:

UNITED STATES DEPARTMENT OF COMMERCE
United States Patent and Trademark Office

September 22, 2003

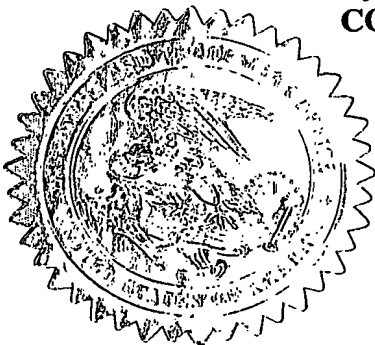
THIS IS TO CERTIFY THAT ANNEXED HERETO IS A TRUE COPY FROM
THE RECORDS OF THE UNITED STATES PATENT AND TRADEMARK
OFFICE OF THOSE PAPERS OF THE BELOW IDENTIFIED PATENT
APPLICATION THAT MET THE REQUIREMENTS TO BE GRANTED A
FILING DATE.

APPLICATION NUMBER: 60/463,965

FILING DATE: April 18, 2003

RELATED PCT APPLICATION NUMBER: PCT/US03/20197

By Authority of the
COMMISSIONER OF PATENTS AND TRADEMARKS



M. Tarver

M. TARVER
Certifying Officer

PRIORITY DOCUMENT
SUBMITTED OR TRANSMITTED IN
COMPLIANCE WITH
RULE 17.1(a) OR (b)

BEST AVAILABLE COPY

04/18/03

31042 U.S. P.T.O.

04-21-02 63965-0114703


the Paperwork Reduction Act of 1995, no persons are required to respond to a collection of information unless it displays a valid OMB control number.

U.S. Patent and Trademark Office; U.S. DEPARTMENT OF COMMERCE

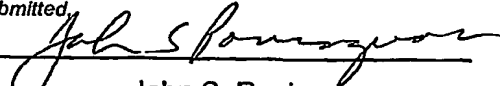
PROVISIONAL APPLICATION FOR PATENT COVER SHEET

This is a request for filing a PROVISIONAL APPLICATION FOR PATENT under 37 CFR 1.53(c).

Express Mail Label No. EL547618608US

INVENTOR(S)					
Given Name (first and middle [if any])		Family Name or Surname		Residence (City and either State or Foreign Country)	
Thomas Neil Dale Conrad		Horsky Jacobson		Boxborough, MA Salem, NH	
<input type="checkbox"/> Additional inventors are being named on the _____ separately numbered sheets attached hereto					
TITLE OF THE INVENTION (500 characters max)					
AN ION IMPLANTATION DEVICE AND A METHOD OF SEMICONDUCTOR MANUFACTURING BY THE IMPLANTATION OF BORON HYDRIDE CLUSTER					
Direct all correspondence to: CORRESPONDENCE ADDRESS					
<input checked="" type="checkbox"/> Customer Number		27160		 Place Customer Number Bar Code Label here PATENT TRADEMARK OFFICE	
OR		Type Customer Number here			
<input type="checkbox"/> Firm or Individual Name		John S. Paniaguas, Katten Muchin Zavis Rosenman			
Address		525 West Monroe Street, Suite 1600			
Address					
City		Chicago	State	Illinois	ZIP 60661-3693
Country		USA	Telephone	312-902-5312	Fax 312-577-4532
ENCLOSED APPLICATION PARTS (check all that apply)					
<input checked="" type="checkbox"/> Specification		Number of Pages 35		<input type="checkbox"/> CD(s), Number	
<input checked="" type="checkbox"/> Drawing(s)		Number of Sheets 26		<input type="checkbox"/> Other (specify)	
<input type="checkbox"/> Application Data Sheet. See 37 CFR 1.76					
METHOD OF PAYMENT OF FILING FEES FOR THIS PROVISIONAL APPLICATION FOR PATENT					
<input checked="" type="checkbox"/> Applicant claims small entity status. See 37 CFR 1.27.				FILING FEE AMOUNT (\$)	
<input checked="" type="checkbox"/> A check or money order is enclosed to cover the filing fees					
<input checked="" type="checkbox"/> The Commissioner is hereby authorized to charge filing fees or credit any overpayment to Deposit Account Number:		50-1214		\$80.00	
<input type="checkbox"/> Payment by credit card. Form PTO-2038 is attached.					
The invention was made by an agency of the United States Government or under a contract with an agency of the United States Government.					
<input checked="" type="checkbox"/> No.					
<input type="checkbox"/> Yes, the name of the U.S. Government agency and the Government contract number are: _____					

Respectfully submitted,

SIGNATURE 

TYPED or PRINTED NAME John S. Paniaguas

TELEPHONE 312-902-5312

Date 01/18/2003

REGISTRATION NO.
(if appropriate)
Docket Number:

31,051
211843-00029

USE ONLY FOR FILING A PROVISIONAL APPLICATION FOR PATENT

This collection of information is required by 37 CFR 1.51. The information is used by the public to file (and by the PTO to process) a provisional application. Confidentiality is governed by 35 U.S.C. 122 and 37 CFR 1.14. This collection is estimated to take 8 hours to complete, including gathering, preparing, and submitting the complete provisional application to the PTO. Time will vary depending upon the individual case. Any comments on the amount of time you require to complete this form and/or suggestions for reducing this burden, should be sent to the Chief Information Officer, U.S. Patent and Trademark Office, U.S. Department of Commerce, Washington, D.C. 20231. DO NOT SEND FEES OR COMPLETED FORMS TO THIS ADDRESS. SEND TO: Box Provisional Application, Assistant Commissioner for Patents, Washington, D.C. 20231.

60163965 . 041803

PROVISIONAL APPLICATION TRANSMITTAL
(37 C.F.R. §1.53(c))

Attorney Docket No. 211843-00029

IN THE UNITED STATES PATENT AND TRADEMARK OFFICE

Box PROVISIONAL PATENT APPLICATION
Commissioner for Patents
Washington, D.C. 20231

Sir:

Transmitted herewith for filing under 37C.F.R. §1.53(c)
is the provisional patent application of:

Title: An Ion Implantation Device and a Method of
Semiconductor Manufacturing
by the Implantation of Boron Hydride Cluster

CERTIFICATE OF MAILING BY "EXPRESS MAIL"

"Express Mail" Mailing Label Number

EL547618608US

Date of Deposit April 18, 2003

I hereby certify that this paper or fee is being deposited with
the United States Postal Service "Express Mail Post Office to
Addressee" Service under 37 CFR §1.10 on the date
indicated above and is addressed to the Commissioner of
Patents and Trademarks, Attention: Assistant Commissioner
for Patents, Washington, D.C. 20231

Benjamin Frey

(Typed or printed name of person mailing)


(Signature of person mailing)

10996 U.S. PTO
60/463965



PROVISIONAL PATENT APPLICATION TRANSMITTAL

Enclosed are:

1. (X) Cover Sheet for the above-identified provisional patent application identifying the application as a provisional application.
2. **Application Papers Enclosed**

# of Specification pages	35		
# of Claim pages	3		
# of Abstract pages	1		
# of Sheets of Drawings	26	() Formal	(X) Informal
3. **Provisional Application Filing Fee**
 - () A check in the amount of \$_____ to cover the filing fee for the above-identified provisional patent application *without* a claim of small entity status.
 - (X) A check in the amount of \$80.00 to cover the filing fee for the above-identified provisional patent application by an entity claiming small entity status.

PROVISIONAL PATENT APPLICATION
211843-00029

4. Method of Payment of Fees

- (X) Enclosed is our firm check in the amount of: \$80.00.
- () Charge \$ _____ to Deposit Account No. 50-1214.
5. () A separate written request under 37 C.F.R. §1.136(a)(3) which is a general authorization to treat any concurrent or future reply requiring a petition for an extension of time under 37 C.F.R. §1.136(a) for its timely submission as incorporating a petition for an extension of time for the appropriate length of time therein.
6. (X) The Commissioner is hereby authorized to charge any additional fees which may be required in this application under 37 C.F.R. §§1.16-1.17 during its entire pendency, or credit any overpayment, to Deposit Account No. 50-1214. Should no proper payment be enclosed herewith, as by a check being in the wrong amount, unsigned, post-dated, otherwise improper or informal or even entirely missing, the Commissioner is authorized to charge the unpaid amount to Deposit Account No. 50-1214. This sheet is filed in triplicate.
7. () Also enclosed:

Please direct all future communications to:

KATTEN MUCHIN ZAVIS ROSENMAN
Attention: Patent Administrator
525 West Monroe Street, Suite 1600
Chicago, Illinois 60661-3693
(312) 577-8134

Respectfully Submitted,

April 18, 2003
(Date)

By: _____

John S. Paniaguas
John S. Paniaguas
Registration No. 31,051

KATTEN MUCHIN ZAVIS ROSENMAN
525 West Monroe Street, Suite 1600
Chicago, Illinois 60661-3693
(Direct) Phone No. (312) 902-5312
(Direct) Fax No. (312) 577-4532

CERTIFICATE OF MAILING BY "EXPRESS MAIL"

"Express Mail Mailing Label Number"

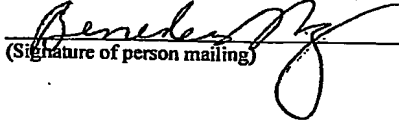
EL547618608US

Date of Deposit April 18, 2003

I hereby certify that this paper or fee is being deposited with the United States Postal Service "Express Mail Post Office to Addressee" Service under 37 CFR §1.10 on the date indicated above and is addressed to the Commissioner for Patents, Washington, D.C. 20231.

Benjamin Frey

(Typed or printed name of person mailing)


(Signature of person mailing)

**AN ION IMPLANTATION DEVICE AND A METHOD OF SEMICONDUCTOR
MANUFACTURING BY THE IMPLANTATION OF BORON HYDRIDE CLUSTER IONS**

Background of the Invention

1. Field of the Invention

The present invention relates to a method of semiconductor manufacturing in which P-type doping is accomplished by the implantation of ion beams formed from ionized boron hydride molecules, said ions being of the form $B_nH_x^+$ and $B_nH_x^-$, where $10 \leq n \leq 100$ and $0 \leq x \leq n+4$.

2. Description of the Prior Art

2.1 The Ion Implantation Process

The fabrication of semiconductor devices involves, in part, the introduction of impurities into the semiconductor substrate to form doped regions. The impurity elements are selected to bond appropriately with the semiconductor material so as to create electrical carriers, thus altering the electrical conductivity of the semiconductor material. The electrical carriers can either be electrons (generated by N-type dopants) or holes (generated by P-type dopants). The concentration of dopant impurities so introduced determines the electrical conductivity of the resultant region. Many such N- and P-type impurity regions must be created to form transistor structures, isolation structures and other such electronic structures, which function collectively as a semiconductor device.

The conventional method of introducing dopants into a semiconductor substrate is by ion implantation. In ion implantation, a feed material containing the desired element is introduced into an ion source and energy is introduced to ionize the feed material, creating ions which contain the dopant element (for example, in silicon the elements ^{75}As , ^{31}P , and ^{121}Sb are *donors* or N-type dopants, while ^{11}B and ^{115}In are *acceptors* or P-type dopants). An accelerating electric field is provided to extract and accelerate the typically positively-charged ions, thus creating an ion beam (in certain cases, negatively-charged ions may be used instead). Then, mass analysis is used to select the species to be implanted, as is known in the art, and the mass-analyzed ion beam may subsequently pass through ion optics which alter its final velocity or change its spatial distribution prior to being directed into a semiconductor substrate or workpiece. The accelerated ions possess a well-defined kinetic energy which allows the ions to penetrate the target to a well-defined, predetermined depth at each energy value. Both the energy and mass of the ions determine their depth of penetration into the target, with higher energy and/or lower mass ions allowing deeper penetration into the target due to their greater velocity. The ion implantation system is constructed to carefully control the critical variables in the implantation process, such as the ion energy, ion mass, ion beam current (electrical charge per unit time), and ion dose at the target (total number of ions per unit area that penetrate into the target). Further, beam angular divergence (the variation in the angles at which the ions strike the substrate) and beam spatial uniformity and extent must also be controlled in order to preserve semiconductor device yields.

A key process of semiconductor manufacturing is the creation of P-N junctions within the semiconductor substrate. This requires the formation of adjacent regions of P-type and N-type doping. An important example of the formation of such a junction is the implantation of P-type dopant into a semiconductor region already containing a uniform distribution of N-type dopant. In this case, an important parameter is the junction depth, which is defined as the depth from the semiconductor surface at which the P-type and N-type dopants have equal concentrations. This junction depth is a function of the implanted dopant mass, energy and dose.

An important aspect of modern semiconductor technology is the continuous evolution to smaller and faster devices. This process is called *scaling*. Scaling is driven by continuous advances in lithographic process methods, allowing the definition of smaller and smaller features in the semiconductor substrate which contains the integrated circuits. A generally accepted scaling theory has been developed to guide chip manufacturers in the appropriate resize of all aspects of the semiconductor device design at the same time, *i.e.*, at each technology or scaling node. The greatest impact of scaling on ion implantation process is the scaling of junction depths, which requires increasingly shallow junctions as the device dimensions are decreased. This requirement for increasingly shallow junctions as integrated circuit technology scales translates into the following requirement: ion implantation energies must be reduced with each scaling step. The extremely shallow junctions called for by modern, sub-0.13 micron devices are termed "Ultra-Shallow Junctions", or USJ.

2.2 Physical Limitations on Low-Energy Beam Transport

Due to the aggressive scaling of junction depths in CMOS processing, the ion energy required for many critical implants has decreased to the point that conventional ion implantation systems, which were originally developed to generate much higher energy beams, deliver much reduced ion currents to the wafer, reducing wafer throughput. The limitations of conventional ion implantation systems at low beam energy are most evident in the extraction of ions from the ion source, and their subsequent transport through the implanter's beam line. Ion extraction is governed by the Child-Langmuir relation, which states that the extracted beam current density is proportional to the extraction voltage (*i.e.*, beam energy at extraction) raised to the $3/2$ power. Fig. 2 is a graph of maximum extracted boron beam current versus extraction voltage. For simplicity, an assumption has been made that only $^{11}\text{B}^+$ ions are present in the extracted beam. Fig. 2 shows that as the energy is reduced, extraction current drops quickly. In a conventional ion implanter, this regime of "extraction-limited" operation is seen at energies less than about 10 keV. Similar constraints affect the transport of the low-energy beam after extraction. A lower energy ion beam travels with a smaller velocity, hence for a given value of beam current the ions are closer together,

i.e., the ion density increases. This can be seen from the relation $J = \eta ev$, where J is the ion beam current density in mA/cm², η is the ion density in ions/cm³, e is the electronic charge ($=6.02 \times 10^{-19}$ Coulombs), and v is the average ion velocity in cm/s. In addition, since the electrostatic forces between ions are inversely proportional to the square of the distance between them, electrostatic repulsion is much stronger at low energy, resulting in increased dispersion of the ion beam. This phenomenon is called "beam blow-up", and is the principal cause of beam loss in low-energy transport. While low-energy electrons present in the implanter beam line tend to be trapped by the positively-charged ion beam, compensating for space-charge blow-up during transport, blow-up nevertheless still occurs, and is most pronounced in the presence of electrostatic focusing lenses, which tend to strip the loosely-bound, highly mobile compensating electrons from the beam. In particular, severe extraction and transport difficulties exist for light ions, such as the P-type dopant boron, whose mass is only 11 amu. Being light, boron atoms penetrate further into the substrate than other atoms, hence the required implantation energies for boron are lower than for the other implant species. In fact, extremely low implantation energies of less than 1 keV are being required for certain leading edge USJ processes. In reality, most of the ions extracted and transported from a typical BF₃ source plasma are not the desired ion $^{11}\text{B}^+$, but rather ion fragments such as $^{19}\text{F}^+$ and $^{49}\text{BF}_2^+$; these serve to increase the charge density and average mass of the extracted ion beam, further increasing space-charge blow-up. For a given beam energy, increased mass results in a greater beam perveance; since heavier ions move more slowly, the ion density η increases for a given beam current, increasing space charge effects in accordance with the discussion above.

2.3 Molecular Ion Implantation

One way to overcome the limitations imposed by the Child-Langmuir relation discussed above is to increase the transport energy of the dopant ion by ionizing a *molecule* containing the dopant of interest, rather than a single dopant atom. In this way, while the kinetic energy of the molecule is higher during transport, upon entering the substrate, the molecule breaks up into its constituent atoms, sharing the energy of the molecule among the individual atoms according to their distribution in mass, so that

the dopant atom's implantation energy is much lower than the original transport kinetic energy of the molecular ion. Consider the dopant atom "X" bound to a radical "Y" (disregarding for purposes of discussion the issue of whether "Y" affects the device-forming process). If the ion XY^+ were implanted in lieu of X^+ , then XY^+ must be extracted and transported at a higher energy, increased by a factor equal to the mass of XY divided by the mass of X ; this ensures that the velocity of X in either case is the same. Since the space-charge effects described by the Child-Langmuir relation discussed above are super-linear with respect to ion energy, the maximum transportable ion current is increased. Historically, the use of polyatomic molecules to ameliorate the problems of low energy implantation is well known in the art. A common example has been the use of the BF_2^+ molecular ion for the implantation of low-energy boron, in lieu of B^+ . This process dissociates BF_3 feed gas to the BF_2^+ ion for implantation. In this way, the ion mass is increased to 49 AMU, allowing an increase of the extraction and transport energy by more than a factor of 4 (*i.e.*, 49/11) over using single boron atoms. Upon implantation, however, the boron energy is reduced by the same factor of (49/11). It is worthy of note that this approach does *not* reduce the current density in the beam, since there is only one boron atom per unit charge in the beam. In addition, this process also implants fluorine atoms into the semiconductor substrate along with the boron, an undesirable feature of this technique since fluorine has been known to exhibit adverse effects on the semiconductor device.

2.4 Cluster Implantation

In principle, a more effective way to increase dose rate than by the XY^+ model discussed above is to implant *clusters* of dopant atoms, that is, molecular ions of the form $X_nY_m^+$, where n and m are integers and n is greater than one. Recently, there has been seminal work using decaborane as a feed material for ion implantation. The implanted particle was a positive ion of the decaborane molecule, $B_{10}H_{14}$, which contains 10 boron atoms, and is therefore a "cluster" of boron atoms. This technique not only increases the mass of the ion and hence the transport ion energy, but for a given ion current, it substantially increases the implanted dose rate, since the decaborane ion $B_{10}H_x^+$ has ten boron atoms. Importantly, by significantly reducing the

electrical current carried in the ion beam (by a factor of 10 in the case of decaborane ions) not only are beam space-charge effects reduced, increasing beam transmission, but wafer charging effects are reduced as well. Since positive ion bombardment is known to reduce device yields by charging the wafer, particularly damaging sensitive gate isolation, such a reduction in electrical current through the use of cluster ion beams is very attractive for USJ device manufacturing, which must increasingly accommodate thinner gate oxides and exceedingly low gate threshold voltages. Thus, there is a critical need to solve two distinct problems facing the semiconductor manufacturing industry today: wafer charging, and low productivity in low-energy ion implantation. The present invention proposes to further increase the benefits of cluster implantation by using significantly larger boron hydride clusters having $n > 10$. In particular, we have implanted the $B_{18}H_x^+$ ion, and further propose to implant the $B_{36}H_x^+$ ion, using the solid feed material octadecaborane, or $B_{18}H_{22}$. We present first results showing that this technology is a significant advance over previous efforts in boron cluster implantation.

2.5. Ion Implantation Systems

Ion implanters have historically been segmented into three basic categories: high current, medium current, and high-energy implanters. Cluster beams are useful for high current and medium-current implantation processes. More particularly, today's high current implanters are primarily used to form the low-energy, high dose regions of the transistor such as drain structures and doping of the polysilicon gates. They are typically batch implanters, *i.e.*, processing many wafers mounted on a spinning disk, the ion beam remaining stationary. Such an exemplary high current implantation system suitable for cluster implantation within the context of the present invention is shown in Fig. 1(a). High current transport systems tend to be simpler than medium-current transport systems, and incorporate a large acceptance of the ion beam. At low energies and high currents, prior art implanters produce a beam at the substrate which tends to be large, with a large angular divergence (*e.g.*, a half-angle up to seven degrees). In contrast, medium-current implanters typically incorporate a serial (one wafer at a time) process chamber, which offers a high tilt capability (*e.g.*, up to 60 degrees from the substrate normal). The ion beam is typically electromagnetically or electrostatically scanned across the wafer at a high frequency, up to about 2 kilohertz in one dimension

(e.g., laterally) and mechanically scanned at a low frequency of less than 1 Hertz in an orthogonal direction (e.g., vertically), to obtain areal coverage and provide dose uniformity over the substrate. Such an exemplary medium-current implantation system suitable for cluster implantation within the context of the present invention is shown in Fig. 1(b). Process requirements for medium-current implants are more complex than those for high-current implants. In order to meet typical commercial implant dose uniformity and repeatability requirements of a variance of only a few per cent, the ion beam must possess excellent angular and spatial uniformity (angular uniformity of beam on wafer of $\leq 1^\circ$, for example). Because of these requirements, medium-current beam lines are engineered to give superior beam control at the expense of reduced acceptance. That is, the transmission efficiency of the ions through the implanter is limited by the emittance of the ion beam. Presently, the generation of higher current (about 1 mA) ion beams at low (< 10 keV) energy is problematic in serial implanters, such that wafer throughput is unacceptably low for certain lower-energy implants (for example, in the creation of source and drain structures in leading-edge CMOS processes). Similar transport problems also exist for batch implanters (processing many wafers mounted on a spinning disk) at the low beam energies of < 5 keV per ion.

While it is possible to design beam transport optics which are nearly aberration-free, the ion beam characteristics (spatial extent, spatial uniformity, angular divergence and angular uniformity) are nonetheless largely determined by the emittance properties of the ion source itself (*i.e.*, the beam properties at ion extraction which determine the extent to which the implanter optics can focus and control the beam as emitted from the ion source). The use of cluster beams instead of monomer beams can significantly enhance the emittance of an ion beam by raising the beam transport energy and reducing the electrical current carried by the beam. However, prior art ion sources for ion implantation are not effective at producing or preserving ionized clusters of the required N- and P-type dopants. Thus, there is a need for cluster ion and cluster ion source technology in order to provide a better-focused, more collimated and more tightly controlled ion beam on target, and in addition to provide higher effective dose rates and higher throughputs in semiconductor manufacturing.

An alternative approach to beam line ion implantation for the doping of semiconductors is so-called "plasma immersion". This technique is known by several other names in the semiconductor industry, such as PLAD (PLASMA Doping), PPLAD (Pulsed PLASMA Doping, and PI³ (Plasma Immersion Ion Implantation). Doping using these techniques requires striking a plasma in a large vacuum vessel that has been evacuated and then backfilled with a gas containing the dopant of choice such as boron trifluoride, diborane, arsine, or phosphine. The plasma by definition has positive ions, negative ions and electrons in it. The target is then biased negatively thus causing the positive ions in the plasma to be accelerated toward the target. The energy of the ions is described by the equation $U = QV$, where U is the kinetic energy of the ions, Q is the charge on the ion, and V is the bias on the wafer. With this technique there is no mass analysis. All positive ions in the plasma are accelerated and implanted into the wafer. Therefore extremely clean plasma must be generated. With this technique of doping a vapor of boron clusters such as $B_{18}H_{22}$, or arsenic clusters such as As_4H_x could be introduced into the vessel and a plasma ignited, followed by the application of a negative bias on the wafer. The bias can be constant in time, time-varying, or pulsed. Dose can be parametrically controlled by knowing the relationship between pressure of the vapor in the vessel, the temperature, the magnitude of the biasing and the duty cycle of the bias voltage and the ion arrival rate on the target. It is also possible to directly measure the current on the target. As with beam line implantation, using octodecaborane there would be an 18 times enhancement in dose rate and 20 times higher accelerating voltages required if octodecaborane were the vapor of choice. If As_4H_x were used there would be a four times dose rate enhancement and a four times the voltage required. There would also be reduced changing as with the beam line implants utilizing clusters.

3. Summary of the Invention

An object of this invention is to provide a method of manufacturing a semiconductor device, this method being capable of forming ultra-shallow impurity-

doped regions of P-type (*i.e.*, acceptor) conductivity in a semiconductor substrate, and furthermore to do so with high productivity.

Another object of this invention is to provide a method of manufacturing a semiconductor device, this method being capable of forming ultra-shallow impurity-doped regions of P-type (*i.e.*, acceptor) conductivity in a semiconductor substrate using ionized clusters of the form $B_nH_x^+$ and $B_nH_x^-$, where $10 < n < 100$ and $0 \leq x \leq n+4$.

A further object of this invention is to provide a method of manufacturing a semiconductor device by implanting ionized molecules of octadecaborane, $B_{18}H_{22}$, of the form $B_{18}H_x^+$ or $B_{18}H_x^-$, where x is an integer less than or equal to 22.

A still further object of this invention is to provide for an ion implantation system for manufacturing semiconductor devices, which has been designed to form ultra shallow impurity-doped regions of either N or P conductivity type in a semiconductor substrate through the use of cluster ions.

According to one aspect of this invention, there is provided a method of implanting cluster ions comprising the steps of: providing a supply of molecules which each contain a plurality of dopant atoms into an ionization chamber, ionizing said molecules into dopant cluster ions, extracting and accelerating the dopant cluster ions with an electric field, selecting the desired cluster ions by mass analysis, modifying the final implant energy of the cluster ion through post-analysis ion optics, and implanting the dopant cluster ions into a semiconductor substrate.

An object of this invention is to provide a method that allows the semiconductor device manufacturer to ameliorate the difficulties in extracting low energy ion beams by implanting a cluster of n dopant atoms ($n = 18$ in the case of $B_{18}H_x^+$) rather than implanting a single atom at a time. The cluster ion implant approach provides the equivalent of a low energy, monatomic implant since each atom of the cluster is implanted with an energy of E/n . Thus, the implanter is operated at an extraction voltage n times higher than the required implant energy, which enables higher ion beam current, particularly at the low implantation energies required by USJ formation. Considering the ion extraction stage, the relative improvement enabled by cluster ion implant can be quantified by evaluating the Child-Langmuir limit. It is recognized that this limit can be approximated by:

$$(1) \quad J_{max} = 1.72 (Q/A)^{1/2} V^{3/2} d^{-2},$$

where J_{max} is in mA/cm², Q is the ion charge state, A is the ion mass in AMU, V is the extraction voltage in kV, and d is the gap width in cm. Fig. 2 is a graph of equation (1) for the case of $^{11}B^+$ with $d = 1.27$ cm. In practice, the extraction optics used by many ion implanters can be made to approach this limit. By extension of equation (1), the following figure of merit, Δ , can be defined to quantify the increase in throughput, or implanted dose rate, for a cluster ion implant relative to monatomic implantation:

$$(2) \quad \Delta = n (U_n / U_1)^{3/2} (m_n / m_1)^{-1/2}.$$

Here, Δ is the relative improvement in dose rate (atoms/sec) achieved by implanting a cluster with n atoms of the dopant of interest at an energy U_n relative to the single atom implant of an atom of mass m_1 at energy U_1 , where $U_1 = \text{eV}$. In the case where U_n is adjusted to give the same dopant implantation depth as the monatomic ($n=1$) case, equation (2) reduces to:

$$(3) \quad \Delta = n^2.$$

Thus, the implantation of a cluster of n dopant atoms has the potential to provide a dose rate n^2 higher than the conventional implant of single atoms. In the case of B_{18}H_x , this maximum dose rate improvement is more than 300. The use of cluster ions for ion implant clearly addresses the transport of low-energy (particularly sub-keV) ion beams. It is to be noted that the cluster ion implant process only requires one electrical charge per cluster, rather than having every dopant atom carrying one electrical charge, as in the conventional case. The transport efficiency (beam transmission) is thus improved, since the dispersive Coulomb forces are reduced with a reduction in charge density. Thus, implanting with clusters of n dopant atoms rather than with single atoms ameliorates basic transport problems in low energy ion implantation and enables a dramatically more productive process.

Enablement of this method requires the formation of the cluster ions. The prior art ion sources used in commercial ion implanters produce only a small fraction of primarily lower-order (e.g., $n=2$) clusters relative to their production of monomers, and hence these implanters cannot effectively realize the low-energy cluster beam implantation advantages listed above. Indeed, the intense plasmas provided by many conventional ion sources rather dissociate molecules and clusters into their component elements. The novel ion source described herein produces cluster ions in abundance due to its use of a "soft" ionization process, namely electron-impact ionization by energetic primary electrons. The ion source of the present invention is designed expressly for the purpose of producing and preserving dopant cluster ions. Instead of striking an arc-discharge plasma to create ions, the ion source of the present invention

uses electron-impact ionization of the process gas by energetic electrons injected in the form of one or more focused electron beams.

4. Description of the Drawings

These and other advantages of the present invention will be readily understood with reference to the following specification and attached drawing wherein:

Fig. 1(a) is a schematic diagram of an exemplary high-current cluster ion implantation system in accordance with the present invention.

Fig. 1(b) is a schematic diagram of the accel-decel electrode used in the implantation system of Fig. 1(a).

Fig. 1(c) is an alternative embodiment of a high-current cluster ion implantation system in accordance with the present invention.

Fig. 1(d) is yet another alternative embodiment of a high-current cluster ion implantation system in accordance with the present invention.

Fig. 1(e) is a schematic diagram of an exemplary medium-current cluster ion implantation system in accordance with the present invention.

Fig. 2 is a graphical diagram illustrating maximum $^{11}\text{B}^+$ beam current vs. extraction energy according to the Child-Langmuir Law of equation (1).

Fig. 3 is a perspective view of an ion source in accordance with the present invention, shown in cutaway to expose internal components.

Fig. 4 is a side view of a portion of the ion source shown in Fig. 3, shown in cutaway with the electron beam and magnetic fields shown superimposed thereupon.

Fig. 5 is a perspective diagram of the cluster ion source of Fig. 3, showing details of the ionization region.

Fig. 6 is a diagram of the 3-zone temperature control system used in the ion source of the present invention.

Fig. 7 is a mechanical drawing of the magnetic yoke assembly, showing the magnetic circuit.

Fig. 7a is a mechanical drawing of the magnetic yoke assembly integrated into the ionization chamber of the ion source of the present invention.

Fig. 7b shows a plot of magnetic flux through a cross-section of the magnetic yoke assembly in the xy plane.

Fig. 8 is a graphical illustration of octadecaborane beam current and vapor pressure, versus vaporizer temperature, using the ion source of the present invention.

Fig. 9 is a graphical illustration of the positive ion mass spectrum of $B_{18}H_{22}$ generated with the ion source of the present invention, collected at high mass resolution.

Fig. 10 is a graphical illustration of the negative ion mass spectrum of $B_{18}H_{22}$ overlaid with a positive ion mass spectrum of $B_{18}H_{22}$, both collected at high mass resolution, and generated with the ion source of the present invention.

Fig. 11 is a graphical illustration of the positive ion mass spectrum of $B_{18}H_{22}$ generated with the ion source of the present invention, collected at low mass resolution.

Fig. 11a is a graphical illustration of the positive mass spectrum of $B_{18}H_{22}$ generated with the ion source of the present invention, collected at highest mass resolution and with an expanded horizontal scale, so that individual ion masses can be resolved.

Fig. 12 is a graphical illustration of $B_{18}H_x^+$ beam current as a function of beam extraction energy, measured near the wafer position by a cluster ion implantation system of the present invention.

Fig. 13 is a graphical illustration of the data of Fig. 10 converted to boron dose rate (using $B_{18}H_x^+$ implantation) as a function of boron implant energy, using a cluster ion implantation system of the present invention.

Fig. 14 is a diagram of a CMOS fabrication sequence during formation of the NMOS drain extension.

Fig. 15 is a diagram of a CMOS fabrication sequence during formation of the PMOS drain extension.

Fig. 16 is a diagram of a semiconductor substrate in the process of manufacturing a NMOS semiconductor device, at the step of N-type drain extension implant.

Fig. 17 is a diagram of a semiconductor substrate in the process of manufacturing a NMOS semiconductor device, at the step of the source/drain implant.

Fig. 18 is a diagram of a semiconductor substrate in the process of manufacturing an PMOS semiconductor device, at the step of P-type drain extension implant.

Fig. 19 is a diagram of a semiconductor substrate in the process of manufacturing a PMOS semiconductor device, at the step of the source/drain implant.

Fig. 20 is a graphical illustration of as-implanted SIMS profiles of boron concentrations from a $B_{18}H_x^+$ ion beam implanted into a silicon wafer, using the present invention.

5. Detailed Description

Fig. 1(a) is a schematic diagram of a cluster ion implantation system of the high-current type in accordance with the present invention. Configurations other than that shown in Fig. 1(a) are possible. In general, the electrostatic optics of ion implanters employ slots (apertures displaying a large aspect ratio in one dimension) embedded in electrically conductive plates held at different potentials, which tend to produce ribbon beams, *i.e.*, beams which are extended in one dimension. This approach has proven effective in reducing space-charge forces, and simplifies the ion optics by allowing the separation of focusing elements in the dispersive (short axis) and non-dispersive (long axis) directions. The cluster ion source 10 of the present invention is coupled with an extraction electrode 220 to create an ion beam 200 which contains cluster ions such as $B_{18}H_x^+$ or As_4^+ . The ions are extracted from an elongated slot in ion source 10, called

the ion extraction aperture, by extraction electrode 220, which also incorporates slot lenses of somewhat larger dimension than those of the ion extraction aperture; typical dimensions of the ion extraction aperture may be, for example, 50mm tall by 8mm wide, but other dimensions are possible. The electrode is an accel-decel electrode in a tetrode configuration, *i.e.*, the electrode extracts ions from the ion source at a higher energy and then decelerates them prior to their exiting the electrode. A schematic diagram of the accel-decel electrode is shown in Fig. 1(b). It is comprised of suppression plate 300 biased by power supply V_s , extraction plate 302 biased by power supply V_f , and ground plate 304, which is at implanter terminal ground (not necessarily earth ground in a decel machine). Ion extraction aperture plate 80 is held unipotential with ionization chamber 44 of ion source 10, which is held at ion source potential by power supply V_a . For the production of positive ions, $V_a > 0$, $V_f < 0$, and $V_s < 0$. For production of negative ions, $V_a < 0$, $V_f = 0$, and $V_s > 0$. For example, to produce 20 keV positive ions, typical voltages would be $V_a = 20$ kV, $V_s = -5$ kV, $V_f = -15$ kV. Note that this means that the actual voltages of the various plates are: extraction aperture plate 80 = 20 kV, suppression plate 300 = -20 kV, extraction plate 302 = -15 kV, ground plate 304 = 0V. For producing negative ions, the power supply voltages are reversed. By using bipolar power supplies, either negative or positive ions may be produced by the novel implanter designs of Fig 1a, 1c, 1d, and 1e. Thus, ions are extracted at higher energy from the ion source, and are decelerated upon leaving the ground plate 304, enabling higher extracted currents and improved focusing and transmission of the resultant ion beam 200.

The ion beam 200 typically contains ions of many different masses, *i.e.*, all of the ion species of a given charge polarity created in the ion source 210. The ion beam 200 then enters an analyzer magnet 230. The analyzer magnet 230 creates a dipole magnetic field within the ion beam transport path as a function of the current in the magnet coils; the direction of the magnetic field is shown as normal to the plane of Fig. 1(a), which is also along the non-dispersive axis of the one-dimensional optics. The analyzer magnet 230 is also a focusing element which forms a real image of the ion extraction aperture (*i.e.*, the optical "object" or source of ions) at the location of the mass resolving aperture 270. Thus, mass resolving aperture 270 has the form of a slot of

similar aspect ratio but somewhat larger dimension than the ion extraction aperture. In one embodiment, the width of resolving aperture 270 is continuously variable to allow selection of the mass resolution of the implanter. This feature is important for maximizing delivered beam current of boron hydride cluster ions, which display a number of ion states separated by one AMU, as for example is illustrated in Fig. 11(a). A primary function of the analyzer magnet 230 is to spatially separate, or disperse, the ion beam into a set of constituent beamlets by bending the ion beam in an arc whose radius depends on the mass-to-charge ratio of the discrete ions. Such an arc is shown in Fig. 1(a) as a beam component 240, the selected ion beam. The analyzer magnet 230 bends a given beam along a radius given by Equation (4) below:

$$(4) \quad R = (2mU)^{1/2} / qB,$$

where R is the bending radius, B is the magnetic flux density, m is the ion mass, U is the ion kinetic energy and q is the ion charge state.

The selected ion beam is comprised of ions of a narrow range of mass-energy product only, such that the bending radius of the ion beam by the magnet sends that beam through mass resolving aperture 270. The components of the beam that are not selected do not pass through the mass-resolving aperture 270, but are intercepted elsewhere. For beams with smaller mass-to-charge ratios m/q 250 than the selected beam 240, for example comprised of hydrogen ions having a mass of 1 or 2 AMU, the magnetic field induces a smaller bending radius and the beam intercepts the inner radius wall 300 of the magnet vacuum chamber, or elsewhere upstream of the mass resolving aperture. For beams with larger mass-to-charge ratios 260 than the selected beam 240, the magnetic field induces a larger bending radius, and the beam strikes the outer radius wall 290 of the magnet chamber, or elsewhere upstream of the mass resolving aperture. As is well established in the art, the combination of analyzer magnet 230 and mass resolving aperture 270 form a mass analysis system which selects the ion beam 240 from the multi-species beam 200 extracted from the ion source 10. The selected beam 240 then passes through a post-analysis acceleration/deceleration electrode 310. This stage 310 can adjust the beam energy to the desired final energy value required for the specific implantation process. For example, in low-energy, high-

dose process higher currents can be obtained if the ion beam is formed and transported at a higher energy and then decelerated to the desired, lower implant ion energy prior to reaching the wafer. The post-analysis acceleration/deceleration lens 310 is an electrostatic lens similar in construction to decel electrode 220. To produce low-energy positive ion beams, the front portion of the implanter is enclosed by terminal enclosure 208 and floated below earth ground. A grounded Faraday cage 205 surrounds the enclosure 208 for safety reasons. Thus, the ion beam can be transported and mass-analyzed at higher energies, and decelerated prior to reaching the workpiece. Since decel electrode 300 is a strong-focusing optic, dual quadrupoles 320 refocus ion beam 240 to reduce angular divergence and spatial extent. In order to prevent ions which have undergone charge-exchange or neutralization reactions between the resolving aperture and the substrate 312 (and therefore do not possess the correct energy) from propagating to substrate 312, a neutral beam filter 310a (or "energy filter") is incorporated within this beam path. For example, the neutral beam filter 310a shown incorporates a "dogleg" or small-angle deflection in the beam path which the selected ion beam 240 is constrained to follow through an applied DC electromagnetic field; beam components which have become electrically neutral or multiply-charged, however, would necessarily not follow this path. Thus, only the ion of interest and with the correct ion energy is passed downstream of the exit aperture 314 of the filter 310a.

Once the beam is shaped by quadrupole pair 320 and filtered by neutral beam filter 310a, the ion beam 240 enters the wafer process chamber 330, also held in a high vacuum environment, where it strikes the substrate 312 which is mounted on a spinning disk 315. Many substrates may be mounted on the disk so that many substrates may be implanted simultaneously, *i.e.*, in batch mode. In a batch system, spinning of the disk provides mechanical scanning in the radial direction, and either vertical or horizontal scanning of the spinning disk is also effected at the same time, the ion beam remaining stationary.

Alternative embodiments of high-current implanters are described in Fig. 1c and Fig. 1d. Fig. 1c describes an accel-decel implanter similar to that described in Fig. 1a, but the beam line has been significantly shortened by removal of dual quadrupoles 320 and neutral beam filter 310a. This results in better beam transmission through the

implanter, and provides for higher beam currents on substrate 312. Fig. 1d discloses a non-accel-decel implanter, i.e., in which the vacuum system of the entire implanter is at earth ground. Thus, in FIG. 1d the decel lens 310 and Terminal enclosure 208 have been deleted relative to the embodiment shown in Fig. 1c. The method of cluster beam implantation delivers very high effective dopant beam currents at sub-keV energies, even without deceleration. Thus, Fig. 1d discloses a cluster-beam implantation system which is greatly simplified and more economical to produce; it also possesses a shorter beam line, increasing transmission of beam to substrate 312.

Figure 1(e) schematically illustrates a proposed medium current implanter which incorporates the present invention. There are many alternative configurations from that which is shown in figure 1(e). Ion beams typically a few centimeters high and less than one centimeter wide are produced in the ion source 400 extracted by the extraction electrode 401 and transported through the analyzer magnet 402 and mass resolving aperture 403. This produces a beam 404 of a specific mass-energy product. Since the energy is fixed by the extraction voltage, typically a single mass passes through the mass analyzer and resolving aperture at a given analyzer magnet 402 field. Equation (4) above describes this process. The boron hydride cluster ion beam exits the mass resolving aperture and enters the accel-decel electrode 405. This electrode is specifically designed to either add energy to the ion beam or reduce the energy of the ion beam. For low energy implants beam transport is enhanced by extracting the beam at a higher energy and then reducing the energy in the deceleration electrode. The Child-Langmuir Law, as illustrated in Fig. 2, limits the current that can be extracted from the ion source. The $U^{3/2}$ dependence of current density limit on energy, where U is the extraction energy, is responsible for increased current at higher extraction energies. For higher energy implants the accel-decel electrode is used to increase the energy of the ion beam to an energy that is above the extraction energy. Extraction energies are typically 20-40 keV, and can be decelerated to less than one keV or accelerated to energies as high as 200 keV for singly charged ions, and as high as 500 keV for multiply charged ions. After acceleration, the beam is transported into a quadrupole lens 406 to refocus the beam after the energy is adjusted by the accel-decel electrode. This step increases the transmission efficiency through the rest of the implanter. If the

beam is allow to expand upon leaving the accel-decel region it will hit the walls of beam line and cause particles to be generated by the beam striking the wall of the beam line 408 as well as not being available for implantation into the target. Next the beam encounters the scanning module 407, which scans the beam in one dimension, typically horizontally. The scan frequency is often in the kiloHertz range. This causes the beam to have a very large angular variation, resulting in the beam striking the target at different angles on different parts of the target. To eliminate this scan induced divergence the beam is directed through a beam collimator 410. Beam collimators are either magnetic or electrostatic and yield a wide parallel beam 409. The collimator also removes ions from the beam which are at a different energy than intended, due to charge-exchange reactions encountered in the beam line. Upon exiting the collimator the beam enters the wafer process chamber 411 and strikes the target 412. Medium current implanters usually process one wafer at a time. This is known in the industry as serial processing. Areal coverage of the wafer is accomplished by translating the wafer in a direction orthogonal to the direction of the beam sweep, for example, in the vertical dimension. The frequency of the vertical is very slow compared to the "fast" scan frequency, having a period of 5-10 or more seconds per cycle. The dose (ions/cm²) on the wafer is controlled by monitoring the beam current in a Faraday cup 413 mounted next to the wafer. Once each scan, at the extreme end of the scan, the beam enters the Faraday cup and is monitored. This allows the beam current to be measured at a rate equal to the scan frequency of the beam, for example 1000 times each second. This signal is then used to control the vertical translation speed in the orthogonal direction to beam scan to obtain a uniform dose across the wafer. In addition, the serial process chamber allows for freedom to orient the wafer relative to the ion beam. Wafers can be rotated during the implant process, and can be by tilted to large angles, as much as 60 degrees to the beam normal.

The use of cluster ion beams such as $B_{18}H_x^+$ or $As_4H_x^+$ allows the beam extraction and transmission to take place at higher energies than would be the case for monomers such as B^+ or As^+ . Upon striking the target, the ion energy is partitioned by mass ratio of the individual, constituent atoms. For $B_{18}H_{22}$ the effective boron energy is 10.8/216.4 of the beam energy, because an average boron atom has a mass of 10.8

amu and the molecule has an average mass of 216.4 amu. This allows the beam to be extracted and transported at 20 times the implant energy. Additionally the dose rate is 18 times higher than for a monomer ion. This results in higher throughput and less charging of the wafer. Wafer charging is reduced because there is only one charge for 18 atoms implanted into the wafer instead of one charge for every atom implanted with a monomer beam.

Figure 3 is a diagram of a cluster ion source 10 and its various components. The details of its construction, as well as its preferred modes of operation, is fully disclosed in U.S. Patent Application No. 10/183,768, "Electron Impact Ion Source", submitted June 26, 2002, inventor T. N. Horsky, herein incorporated by reference. The ion source 10 is one embodiment of a novel electron impact ionization source. Figure 3 is a cross-sectional schematic diagram of the source construction which serves to clarify the functionality of the components which make up the ion source 10. The ion source 10 is made to interface to an evacuated vacuum chamber of an ion implanter or other process tool by way of a mounting flange 36. Thus, the portion of the ion source 10 to the right of flange 36, shown in Fig. 3, is at high vacuum (pressure $< 1 \times 10^{-4}$ Torr). Gaseous material is introduced into ionization chamber 44 in which the gas molecules are ionized by electron impact from electron beam 70, which enters the ionization chamber 44 through electron entrance aperture 70a such that electron beam 70 is aligned with ion extraction aperture 81, and exits ionization chamber 44 through electron exit aperture 71. After leaving ionization chamber 44, the electron beam is stopped by beam dump 72 located external to ionization chamber 44. Thus, ions are created adjacent to the ion extraction aperture 81, which appears as a slot in the ion extraction aperture plate 80. The ions are then extracted and formed into an energetic ion beam by an extraction electrode (not shown) located in front of the ion extraction aperture plate 80. The ionization region is shown in more detail in Fig. 4 and in Fig. 5.

Gases may be fed into the ionization chamber 44 via a gas conduit 33. Solid feed materials can be vaporized in a vaporizer 28, and the vapor fed into the ionization chamber 44 through a vapor conduit 32 within the source block 35. Solid feed material 29, located under a perforated separation barrier 34a, is held at a uniform temperature by temperature control of the vaporizer housing 30. Vapor 50 which accumulates in a

ballast volume 31 feeds through conduit 39 and through one or more shutoff valves 100 and 110. The nominal pressure of vapor 50 within shutoff valve 110 is monitored by capacitance manometer gauge 60. The vapor 50 feeds into the ionization chamber 44 through a vapor conduit 32, located in the source block 35. Thus, both gaseous and solid dopant-bearing materials may be ionized by this ion source.

Fig. 4 is a cross-sectional side view which illustrates the fundamental optical design of an electron-beam ion source configuration in accordance with the present invention. In one embodiment of the invention, an electron beam 70 is emitted from a heated filament 110 and executes a 90 degree trajectory due to the influence of beam steerers or static magnetic field B 135 (in a direction normal to the plane of the paper as indicated) into the ionization chamber 44, passing first through base plate aperture 106 in base plate 105, and then through electron entrance aperture 70a in ionization chamber 44. Electrons passing all the way through ionization chamber 44 (*i.e.*, through electron entrance aperture 70a and electron exit aperture 71) are intercepted by a beam dump 72. Emitter shield 102 is unipotential with base plate 105 and provides electrostatic shielding for the propagating electron beam 70. As electron beam 70 propagates through the base plate aperture 106, it is decelerated prior to entering ionization chamber 44 by the application of a voltage V_a to base plate 105 (provided by positive-going power supply 115), and voltage V_c to the filament 135 (provided by negative-going power supply 116), both biased relative to the ionization chamber 44. It is important to maintain an electron beam energy significantly higher than typically desired for ionization in the beam-forming and the transport region, *i.e.*, outside of ionization chamber 44. This is due to the space charge effects which severely reduce the beam current and enlarge the electron beam diameter at low energies. Thus, it is desired to maintain the electron beam energy between about 1.5 keV and 5 keV in this region.

Voltages are all relative to the ionization chamber 44. For example, if $V_c = -0.5$ kV and $V_a = 1.5$ kV, the energy of the electron beam is therefore given by $e(V_a - V_c)$, where e is the electronic charge (6.02×10^{-19} Coulombs). Thus, in this example, the electron beam 70 is formed and deflected at an energy of 2 keV, but upon entering electron entrance aperture 70a, it has an energy of only 0.5 keV.

In one embodiment, a uniform magnetic field $B' 119$ is established within ionization chamber 44 by the incorporation of a permanent magnetic yoke assembly 500, shown in Fig. 7, into ionization chamber 44. Referring now to Fig. 7, magnetic flux is generated by permanent samarium-cobalt magnets 510a and 510b and returned through yoke assembly 500 through the gap between poles 520a and 520b. Electron beam 70 enters through hole 530a in yoke 520a and exits through hole 530b in yoke 520b. Fig. 7b shows how yoke assembly 500 integrates into ionization chamber 44. In Fig. 7a, ionization chamber 44 has a milled-out section which receives yoke assembly 500 and poles 520a and 520b such that the surface 550 of yoke assembly 500 and the surface of ionization chamber 44 are flush. The interior wall of the narrow annulus 540a and 540b (not shown), machined as part of ionization chamber 44, defines electron entrance aperture 70a and electron exit aperture 71, insuring that the ferromagnetic material of yoke assembly 500 is not exposed to the electron beam, reducing any possibility of ferrous metals contamination within the ionization volume of ionization chamber 44. Fig. 7b shows lines of flux along a cross-section containing the xy plane (x is horizontal, y is vertical, antiparallel to the direction of propagation of electron beam 70 as shown in Fig. 5) of yoke assembly 500, calculated with field modeling software. Very uniform field lines 119 are generated within the propagation volume of electron beam 70. $B' 119$ is directed parallel to incoming electron beam 70 in order to confine electron beam 70. Use of a confining magnetic field helps to counteract dispersive space-charge forces which would blow up electron beam 70 subsequent to deceleration, *i.e.*, as it enters ionization chamber 44. This has the benefit of enabling higher charge density in electron beam 70, hence higher ion density near to the preferred ionization region adjacent to ion extraction aperture 81, resulting in increased ion current 120. Further gains may be realized by biasing beam dump 72 to a negative voltage V_r , relative to ionization chamber 44, by power supply 117. For example, if $V_r = V_c$, then a reflex mode may be established, whereby primary electrons contained in electron beam 70 are reflected from beam dump 72, increasing the effective path length of the electrons. At sufficiently low electron energies, the presence of confining field $B' 119$ causes the reflected electrons to execute a helical trajectory along the direction of B' . We note that $B 135$ and $B' 119$ are orthogonal in direction, $B 135$ deflecting the electron

beam 70 into ionization chamber 44 and B' 119 confining the resultant beam; therefore magnetic shield 118 is added to the bottom of base plate 105. Magnetic shield 118 is made of high-permeability metal so as to prevent the two fields from mixing; this separates the path of electron beam 70 into two regions of magnetic field; outside ionization chamber 44, and within ionization chamber 44.

Other elements shown in Fig. 4 include an extracted ion beam 120, a source electrostatic shield 101, and emitter shield 102. Emitter shields 102 shields the electron beams 70 from fields associated with the potential difference between base plate 105 and the source shield 101, which is unipotential with ionization chamber 44. The source shield 101 shields the ion beam 120 from fields generated by the potential difference between base plate 105 and ionization chamber 44, and also acts to absorb stray electrons and ions which may otherwise impact the ion source elements. For this reason, emitter shields 102 and the source shield 101 are constructed of refractory metal, such as molybdenum. Alternatively, more complete shielding of the ion beam 120 from magnetic fields B 135 and B' 119 may be accomplished by fabricating source shield 101 of a ferromagnetic substance, such as magnetic stainless steel.

FIG. 5 is a cutaway view illustrating the mechanical detail and which shows explicitly how the contents of Fig. 4 are incorporated into the ion source of Fig. 3. Electrons are thermionically emitted from filament 110 and accelerated to anode 140, forming electron beam 70. Since electron beam 70 is generated external to the ionization chamber, the emitter life is extended relative to known configurations, since the emitter is in the low-pressure environment of the implanter vacuum housing in which the ion source resides, and since the emitter is also effectively protected from ion bombardment.

Magnetic flux from permanent magnet 130 and magnetic pole assembly 125 is used to steer the beam by establishing a uniform magnetic field across the air gap between the ends of the magnetic pole assembly 125, wherein the electron beam 70 propagates. The magnetic field B 135 and the electron beam energies of electron beam 70 are matched such that electron beam 70 is deflected through approximately 90 degrees, and passes into ionization chamber 44 as shown. By deflecting electron beam

70 for example, through 90 degrees, no line of sight exists between emitter 110 and ionization chamber 44 which contains the ions, thus preventing bombardment of the emitters by energetic charged particles.

Since V_a is positive relative to the ionization chamber 44, electron beam 70 is decelerated as it passes through the gap defined by base plate aperture 106 and electron entrance aperture 70a. Thus, the combination of base plate aperture 106 and electron entrance aperture 70a and the gap between them, forms an electrostatic lens, in this case, a decelerating lens. The use of a decelerating lens allows the ionization energy of the electron beam to be adjusted without substantially affecting the electron beam generation and deflection.

The gap may be established by one or more ceramic spacers 132, which support base plate 105 and act as a stand off from source block 35, which is at ionization chamber potential. The ceramic spacers 132 provide both electrical isolation and mechanical support. Note that for clarity, the emitter shields 102 and the source shield 101 are not shown in Fig. 5. Also not shown is the magnetic yoke assembly which is shown in Fig 7.

Since electron entrance aperture 106 can limit transmission of electron beam 70, base plate 105 can intercept a significant portion of the energetic electron beam 70. base plate 105 must therefore be either actively cooled, or passively cooled. Active cooling may be accomplished by passing liquid coolant, such as water, through base plate 105, or forcing compressed air to flow through said base plate 105. In an alternative embodiment, passive cooling is accomplished by allowing base plate 105 to reach a temperature whereby they cool through radiation to their surroundings. This steady-state temperature depends on the intercepted beam power, the surface area and emissivity of the base plate, and the temperatures of surrounding components. Allowing the base plate 105 to operate at elevated temperature, for example at 250C, is advantageous when running condensable gases which can form contaminating and particle-forming films on exposed cold surfaces.

One aspect of the ion source of the present invention is user control of the ionization chamber temperature, as well as the temperature of the source block and

valves. This feature is advantageous when vaporizing condensable gases, preventing significant coating of surfaces with condensed material, and ensuring efficient transport of the vapor through conduit 39, valves 100, 110, and vapor feed 32. The source utilizes a combination of heating and cooling to achieve accurate control of the source temperature. Separate temperature control is provided for vaporizer 28, shutoff valves 100 and 110, and source block 35. Ionization chamber 44 is passively heated, as is extraction aperture plate 80, by interactions with electron beam 70, and maintains stable operating temperature through thermally conductive interfaces between source block 35 and ionization chamber 44, and between ionization chamber 44 and extraction aperture plate 80, such that source block temp < ionization chamber temp < extraction aperture temp. External electronic controllers (such as an Omron model E5CK) are used for temperature control. Heating is provided by embedded resistive heaters, whose heating current is controlled by the electronic controller. Cooling is provided by a combination of convective and conductive gas cooling methods, as further described, for example, in commonly owned PCT application US01/18822, and in U.S. Application number 10/183,768, both herein incorporated by reference.

Fig. 6 illustrates a closed-loop control system for three independent temperature zones, showing a block diagram of a preferred embodiment in which three temperature zones are defined: zone 1 for vaporizer body 30, zone 2 for isolation valves 100 and 110, and zone 3 for the source block 35. Each zone may have a dedicated controller, for example, an Omron E5CK Digital Controller. In the simplest case, heating elements alone are used to actively control temperature above room ambient, for example, between 18C to 200C or higher. Thus, resistive cartridge-type heaters can be embedded into the vaporizer body 30 (heater 1) and the source block 35 (heater 3), while the valves 100, 110 can be wrapped with silicone strip heaters (heater 2) in which the resistive elements are wire or foil strips. Three thermocouples labeled TC1, TC2, and TC3 in FIG. 6 can be embedded into each of the three components 30, 35, 100 (110) and continuously read by each of the three dedicated temperature controllers. The temperature controllers 1, 2, and 3 are user-programmed with a temperature setpoint SP1, SP2, and SP3, respectively. In one embodiment, the temperature setpoints are such that $SP3 > SP2 > SP1$. For example, in the case where the vaporizer

temperature is desired to be at 30C, SP2 might be 50C and SP3 70C. The controllers typically operate such that when the TC readback does not match the setpoint, the controller's comparator initiates cooling or heating as required. For example, in the case where only heating is used to vary temperature, the comparator output is zero unless $TC1 < SP1$. The controllers may contain a look-up table of output power as a nonlinear function of temperature difference $SP1 - TC1$, and feed the appropriate signals to the controller's heater power supply in order to smoothly regulate temperature to the programmed setpoint value. A typical method of varying heater power is by pulse-width modulation of the power supply. This technique can be used to regulate power between 1% and 100% of full scale. Such PID controllers can typically hold temperature setpoint to within 0.2C.

The method herein described can be considered normal operation of the ion source of the present invention where the only difference from other operational modes is the user's choice of values for the source parameters (feed material, feed gas flow rate, electron ionization energy and current, and source component temperature(s)). We have used solid octadecaborane, $B_{18}H_{22}$, to produce copious amounts of boron hydride cluster ions of the form $B_{18}H_x^+$, by using the vaporizer and ion source depicted in Fig. 3. Octadecaborane is a stable solid at room temperature and has a vapor pressure of a few millitorr. We believe that this material has never before been used in ion implantation. In order to generate useful mass flows of about 1 sccm of octadecaborane vapor 32, the vaporizer 28 was held at about 90C. Fig. 8 displays a plot of two variables as a function of vaporizer temperature: vaporizer pressure on the right vertical axis, and ion current delivered to the post-analysis Faraday cup of a high-current implanter similar to that depicted in Fig. 1d. Referring now to Fig. 3, the vaporizer pressure was measured by capacitance manometer 60 in communication with valve 110. Typical source operating parameters were: valve (100 and 110) temperature = 120C, source block 35 temperature = 120C, electron ionization energy = 1 keV, electron current \approx 70 mA. This was achieved by setting $V_c = -1$ kV, $V_a = 1.3$ kV, $V_r = -1$ kV, and filament emission current = 160 mA.

Fig. 9 shows an octadecaborane mass spectrum collected under similar conditions to those used to generate Fig. 8, in a cluster ion implantation system similar

to that disclosed in Fig. 1d. The variable resolving aperture 270 was set to a high mass resolution, which selected a four-AMU wide ion beam 240 to a downstream Faraday cup. Fig. 10 shows an octadecaborane mass spectra for both negative and positive ions, collected under conditions similar to those used to generate the data of Fig. 9. The polarity of all the implanter power supplies were reversed to switch between negative and positive ions, which were collected within a few minutes of one another and recorded on the same plot. Fig. 10 is a reproduction of that plot without alteration in mass scale or vertical scale. It is of note that the $B_{18}H_x^+$ and $B_{18}H_x^-$ peaks are at 210 AMU. Fig. 11 was collected under conditions similar to those used to collect the data of Fig. 9, but with the resolving aperture 270 set to allow about 18 AMU to pass downstream, allowing much higher $B_{18}H_x^+$ currents. However, the lack of structure in the main peak attests to reduced mass resolution. Fig. 11a is a detail collected at highest mass resolution. With the resolving aperture set at < 1 mm, only a single AMU was passed downstream to the Faraday. Thus, individual boron hydride peaks separated by one AMU are clearly visible. Fig. 12 shows a plot of beam current at the Faraday versus extraction voltage without any deceleration of the ion beam, collected at the low mass resolution of Fig. 11. Fig. 13 shows the data of Fig. 12 converted to atomic boron current versus effective implant energy, as a means of comparison with monomer boron implantation. Atomic boron current = $18 \times$ octadecaborane Faraday current, and effective implant energy = $11/210 \times$ extraction voltage. These currents are many times greater than currently attainable with conventional monomer boron implantation, particularly without ion deceleration.

In order to characterize the implantation profile of $B_{18}H_x^+$ for boron doping of semiconductors, a commercial silicon wafer was dipped in HF solution to remove any native oxide, and implanted in a cluster ion implantation system similar to that disclosed in Fig. 1d. A boron dose of $2 \times 10^{16} \text{ cm}^{-2}$ was delivered by implanting a $B_{18}H_x^+$ dose of $1.1 \times 10^{15} \text{ cm}^{-2}$. The $B_{18}H_x^+$ ion energy was 20 keV during the implant, which means the effective boron implant energy was about 1 keV per boron atom. Figure 20 shows the as-implanted boron profile as determined by SIMS (Secondary Ion Mass Spectrometry). The peak of the profile is at about 50 Å, which agrees well with a projected range of 58 Å predicted by TRIM calculations for a 1 keV boron implant.

An important application of this method is the use of cluster ion implantation for the formation of N- and P-type shallow junctions as part of a CMOS fabrication sequence. CMOS is the dominant digital integrated circuit technology in current use and its name denotes the formation of both N-channel and P-channel MOS transistors (Complementary MOS: both N and P) on the same chip. The success of CMOS is that circuit designers can make use of the complementary nature of the opposite transistors to create a better circuit, specifically one that draws less active power than alternative technologies. It is noted that the N and P terminology is based on Negative and Positive (N-type semiconductor has negative majority carriers, and vice versa), and the N-channel and P-channel transistors are duplicates of each other with the type (polarity) of each region reversed. The fabrication of both types of transistors on the same substrate requires sequentially implanting an N-type impurity and then a P-type impurity, while protecting the other type of devices with a shielding layer of photoresist. It is noted that each transistor type requires regions of both polarities to operate correctly, but the implants which form the shallow junctions are of the same type as the transistor: N-type shallow implants into N-channel transistors and P-type shallow implants into P-channel transistors. An example of this process is shown in Figs. 14 and 15. In particular, Fig. 14 illustrates a method for forming the N-channel drain extension 89 through an N-type cluster implant 88, while Fig. 15 shows the formation of the P-channel drain extension 90 by a P-type cluster implant 91. It is to be noted that both N- and P-types of transistors requires shallow junctions of similar geometries, and thus having both N-type and P-type cluster implants is advantageous for the formation of advanced CMOS structures.

An example of the application of this method is shown in Fig. 16 for the case of forming an NMOS transistor. This figure shows semiconductor substrate 41 which has undergone some of the front-end process steps of manufacturing a semiconductor device. The structure consists of a N-type semiconductor substrate 41 that has been processed through the P-well 43, trench isolation 42, and gate stack formation 44, 45 steps. The P-well 43 forms a junction with the N-type substrate 41 that provides junction isolation for the transistors in the well. The trench isolation 42 provides lateral dielectric isolation between the N- and P- wells (*i.e.*, in the overall CMOS structure).

The gate stack is then constructed, containing the gate oxide layer 44 and the polysilicon gate electrode 45, which have been patterned to form the transistor gate stack. Also, photoresist 46 has been applied and patterned such that the area for NMOS transistors is open, but other areas of the substrate are shielded by the photoresist layer 46. At this point in the process flow, the substrate is ready for the drain extension implant, which is the shallowest doping layer required by the device fabrication process. A typical process requirement for leading-edge devices of the 0.13 μm technology node is an arsenic implant energy of between 1 keV and 2 keV, and an arsenic dose of $5 \times 10^{14} \text{ cm}^{-2}$. The cluster ion beam 47, As_4H_x^+ in this case, is directed at the semiconductor substrate, typically such that the direction of propagation of the ion beam is normal to the substrate, to avoid shadowing by the gate stack. The energy of the As_4H_x^+ cluster should be four times the desired As^+ implant energy, e.g., between 4 keV and 8 keV. The clusters dissociate upon impact with the substrate, and the dopant atoms come to rest in a shallow layer near the surface of the semiconductor substrate, which forms the drain extension region 48. We note that the same implant enters the surface layer of the gate electrode 49, providing additional doping for the gate electrode. The process described in Fig. 16 is thus one important application of the proposed invention.

A further example of the application of this method is shown in Fig. 17: the formation of the deep source/drain regions. This figure shows the semiconductor substrate 41 of Fig. 16 after execution of further processes steps in the fabrication of a semiconductor device. The additional process steps include the formation of a pad oxide 51 and the formation of spacers 52 on the sidewalls of the gate stack. At this point, a photoresist layer 53 is applied and patterned to expose the transistor to be implanted, an NMOS transistor in this example. Next, the ion implant to form the source and drain regions 55 is performed. Since this implant requires a high dose at low energy, it is an appropriate application of the proposed cluster implantation method. Typical implant parameters for the 0.13 μm technology node are approximately 6 keV per arsenic atom (54) at an arsenic dose of $5 \times 10^{15} \text{ cm}^{-2}$, so it requires a 24 keV, $1.25 \times 10^{15} \text{ cm}^{-2}$ As_4H_x^+ implant, a 12 keV, $2.5 \times 10^{15} \text{ cm}^{-2}$ As_2H_x^+ implant, or a 6 keV, $5 \times 10^{15} \text{ cm}^{-2}$ As^+ implant. As shown in Fig. 16, the source and drain regions 55 are

formed by this implant. These regions provide a high conductivity connection between the circuit interconnects (to be formed later in the process) and the intrinsic transistor defined by the drain extension 48 in conjunction with the channel region 56 and the gate stack 44, 45. It may be noted that the gate electrode 45 can be exposed to this implant (as shown), and if so, the source/drain implant provides the primary doping source for the gate electrode. This is shown in Fig. 17 as the poly doping layer 57.

The detailed diagrams showing the formation of the PMOS drain extension 148 and PMOS source and drain regions 155 are shown in Figs 18 and 19, respectively. The structures and processes are the same as in Figs. 17 and 18 with the dopant types reversed. In Fig 18, the PMOS drain extension 148 is formed by the implantation of a boron cluster implant 147. Typical parameters for this implant would be an implant energy of 500eV per boron atom with a dose of $5 \times 10^{14} \text{ cm}^{-2}$, for the 0.13um technology node. Thus, a $\text{B}_{18}\text{H}_x^+$ implant at 211 AMU would be at 9.6 keV at an octadecaborane dose of $2.8 \times 10^{13} \text{ cm}^{-2}$. Fig. 19 shows the formation of the PMOS source and drain regions 148, again by the implantation of a P-type cluster ion beam 154 such as octadecaborane. Typical parameters for this implant would be an energy of around 2keV per boron atom with a boron dose of $5 \times 10^{15} \text{ cm}^{-2}$ (i.e., 38.4 keV octadecaborane at $2.8 \times 10^{14} \text{ cm}^{-2}$) for the 0.13um technology node.

In general, ion implantation alone is not sufficient for the formation of an effective semiconductor junction: a heat treatment is necessary to electrically activate the implanted dopants. After implantation, the semiconductor substrate's crystal structure is heavily damaged (substrate atoms are moved out of crystal lattice positions), and the implanted dopants are only weakly bound to the substrate atoms, so that the implanted layer has poor electrical properties. A heat treatment, or anneal, at high temperature (greater than 900C) is typically performed to repair the semiconductor crystal structure, and to position the dopant atoms substitutionally, i.e., in the position of one of the substrate atoms in the crystal structure. This substitution allows the dopant to bond with the substrate atoms and become electrically active; that is, to change the conductivity of the semiconductor layer. This heat treatment works against the formation of shallow junctions, however, because diffusion of the implanted dopant occurs during the heat treatment. Boron diffusion during heat treatment, in fact, is the limiting factor in

achieving USJ's in the sub-0.1 micron regime. Advanced processes have been developed for this heat treatment to minimize the diffusion of the shallow implanted dopants, such as the "spike anneal". The spike anneal is a rapid thermal process wherein the residence time at the highest temperature approaches zero: the temperature ramps up and down as fast as possible. In this way, the high temperatures necessary to activate the implanted dopant are reached while the diffusion of the implanted dopants is minimized. It is anticipated that such advanced heat treatments would be utilized in conjunction with the present invention to maximize its benefits in the fabrication of the completed semiconductor device.

Obviously, many modifications and variations of the present invention are possible in light of the above teachings. Thus, it is to be understood that, within the scope of the appended claims, the invention may be practiced otherwise than as specifically described above.

What is claimed and desired to be covered by a Letters Patent is as follows:

Claims

1. A method of implanting ions comprising the steps of: producing a volume of gas phase molecules of a boron hydride B_nH_m , where n and m are integers and $n > 10$ and $m \geq 0$;

ionizing the boron hydride molecules; and

accelerating the boron hydride ions by an electric field to implant into a target, to perform doping of a semiconductor.

2. The method of claim 1, in which the boron hydride is Octadecaborane, $B_{18}H_{22}$.
3. The method of claim 2, in which said ion is $B_{18}H_x^+$, and $0 \leq x \leq 22$.
4. The method of claim 2, in which said ion is $B_{36}H_y^+$, and $0 \leq y \leq 44$.
5. The method of claim 2, in which said ion is $B_{18}H_x^-$, and $0 \leq x \leq 22$.
6. The method of claim 2, in which said ion is $B_{36}H_y^-$, and $0 \leq y \leq 44$.
7. The method of claim 1, in which said gas phase B_nH_m is produced by sublimation of a solid by heating above 20C.
8. The method of claim 1, wherein said gas phase B_nH_m is introduced into an ion source for ionization.
9. The method of claim 8, wherein said ion source is incorporated into an ion implanter.
10. The method of claim 1, wherein said target is silicon.

11. The method of claim 1, wherein said target is a silicon-on-insulator substrate.
12. The method of claim 1, wherein said target is a strained superlattice substrate.
13. The method of claim 12, wherein said substrate comprises a Silicon Germanium (SiGe) strained superlattice.
14. A method of implanting ions comprising the steps of: producing a volume of gas phase molecules of a boron hydride B_nH_m , where n and m are integers and $n > 10$ and $m \geq 0$;

forming a plasma containing boron hydride molecules, boron hydride ions and electrons; and

accelerating the boron hydride ions by an electric field to implant into a target, to perform doping of a semiconductor.
15. The method of claim 14, wherein said electric field is a time-varying or pulsed electric field.
16. The method of claim 14, wherein said electric field is a constant or DC electric field.
17. The method of claim 14, in which said boron hydride is Octadecaborane, $B_{18}H_{22}$.
18. The method of claim 14, in which said boron hydride ion is $B_{18}H_x^+$, and $0 \leq x \leq 22$.
19. The method of claim 14, in which said gas phase B_nH_m is produced by sublimation of a solid by heating above 20C.
20. The method of claim 14, wherein said target is silicon.

21. The method of claim 14, wherein the target is a silicon-on-insulator substrate.
22. The method of claim 14, wherein said target is a strained superlattice substrate.
23. The method of claim 22, wherein said substrate comprises a Silicon Germanium (SiGe) strained superlattice.

ABSTRACT

AN ION IMPLANTATION DEVICE AND A METHOD OF SEMICONDUCTOR MANUFACTURING BY THE IMPLANTATION OF BORON HYDRIDE CLUSTER IONS

An ion implantation device and a method of manufacturing a semiconductor device is described, wherein ionized boron hydride molecular clusters are implanted to form P-type transistor structures. For example, in the fabrication of Complementary Metal-Oxide Semiconductor (CMOS) devices, the clusters are implanted to provide P-type doping for Source and Drain structures and for Poly gates; these doping steps are critical to the formation of PMOS transistors. The molecular cluster ions have the chemical form $B_nH_x^+$ and $B_nH_x^-$, where $10 < n < 100$ and $0 \leq x \leq n+4$. The use of such boron hydride clusters results in a dramatic increase in wafer throughput, as well as improved device yields through the reduction of wafer charging. Thus, this technology significantly reduces manufacturing costs relative to prior implantation techniques.

A method of manufacturing a semiconductor device is further described, comprising the steps of: providing a supply of molecules containing a plurality of dopant atoms into an ionization chamber, ionizing said molecules into dopant cluster ions, extracting and accelerating the dopant cluster ions with an electric field, selecting the desired cluster ions by mass analysis, modifying the final implant energy of the cluster ion through post-analysis ion optics, and implanting the dopant cluster ions into a semiconductor substrate. In general, dopant molecules contain n dopant atoms, where n is an integer number greater than 10. This method enables increasing the dopant dose rate to n times the implantation current with an equivalent per dopant atom energy of $1/n$ times the cluster implantation energy, while reducing the charge per dopant atom by the factor n . This is an effective method for making shallow transistor junctions, where it is desired to implant with a low energy per dopant atom.

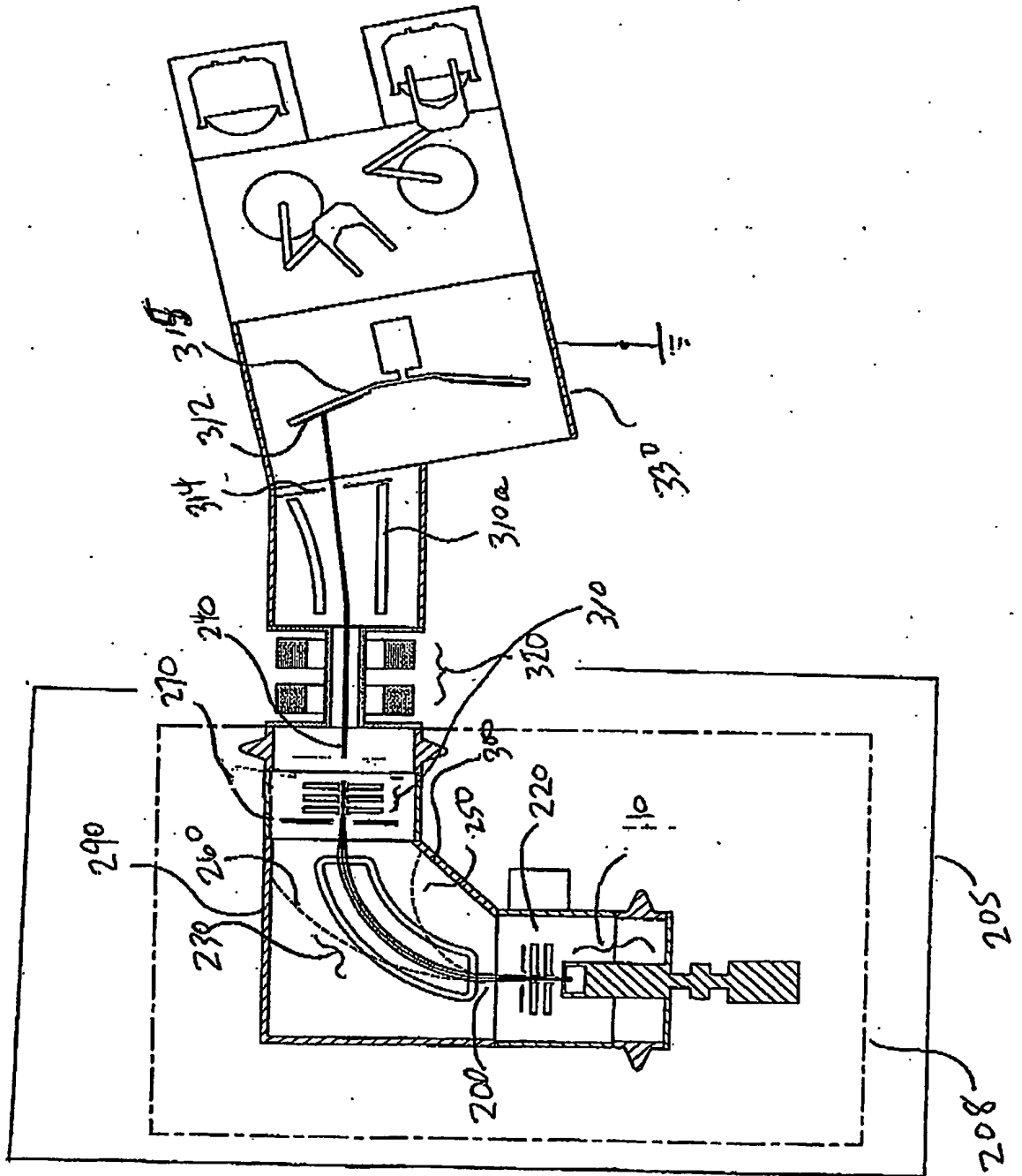


Fig. 1 (a)

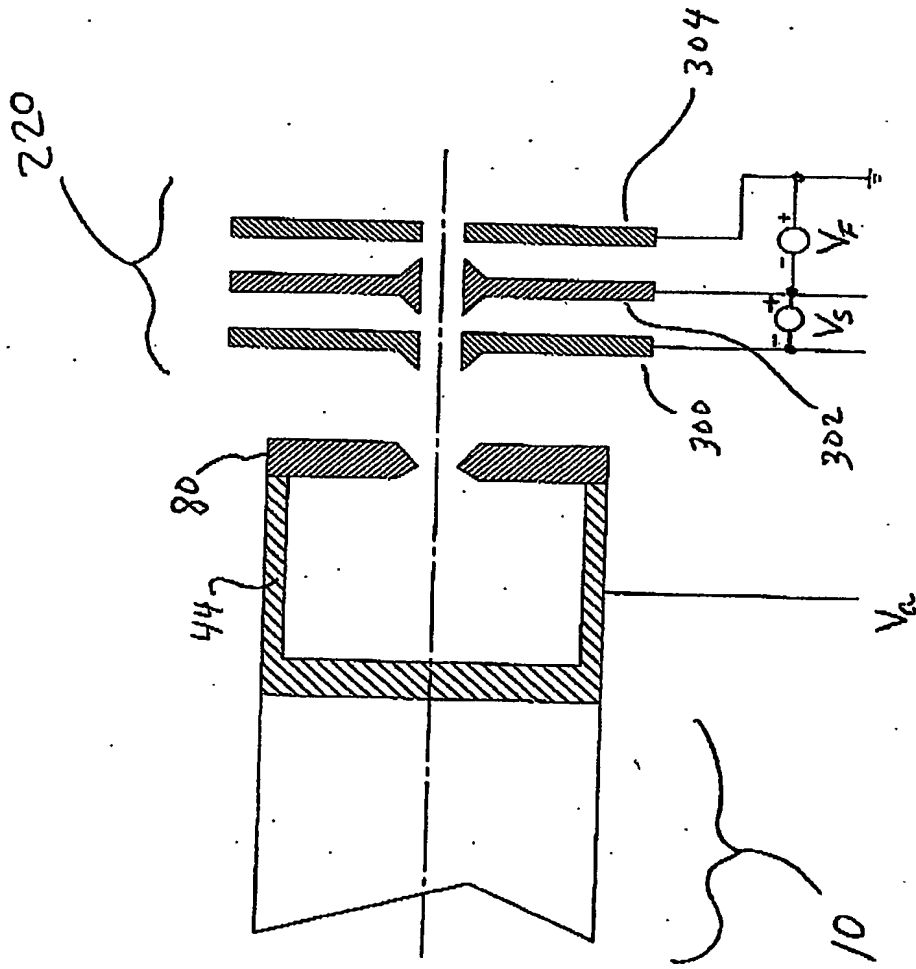


Fig. 1 (b)

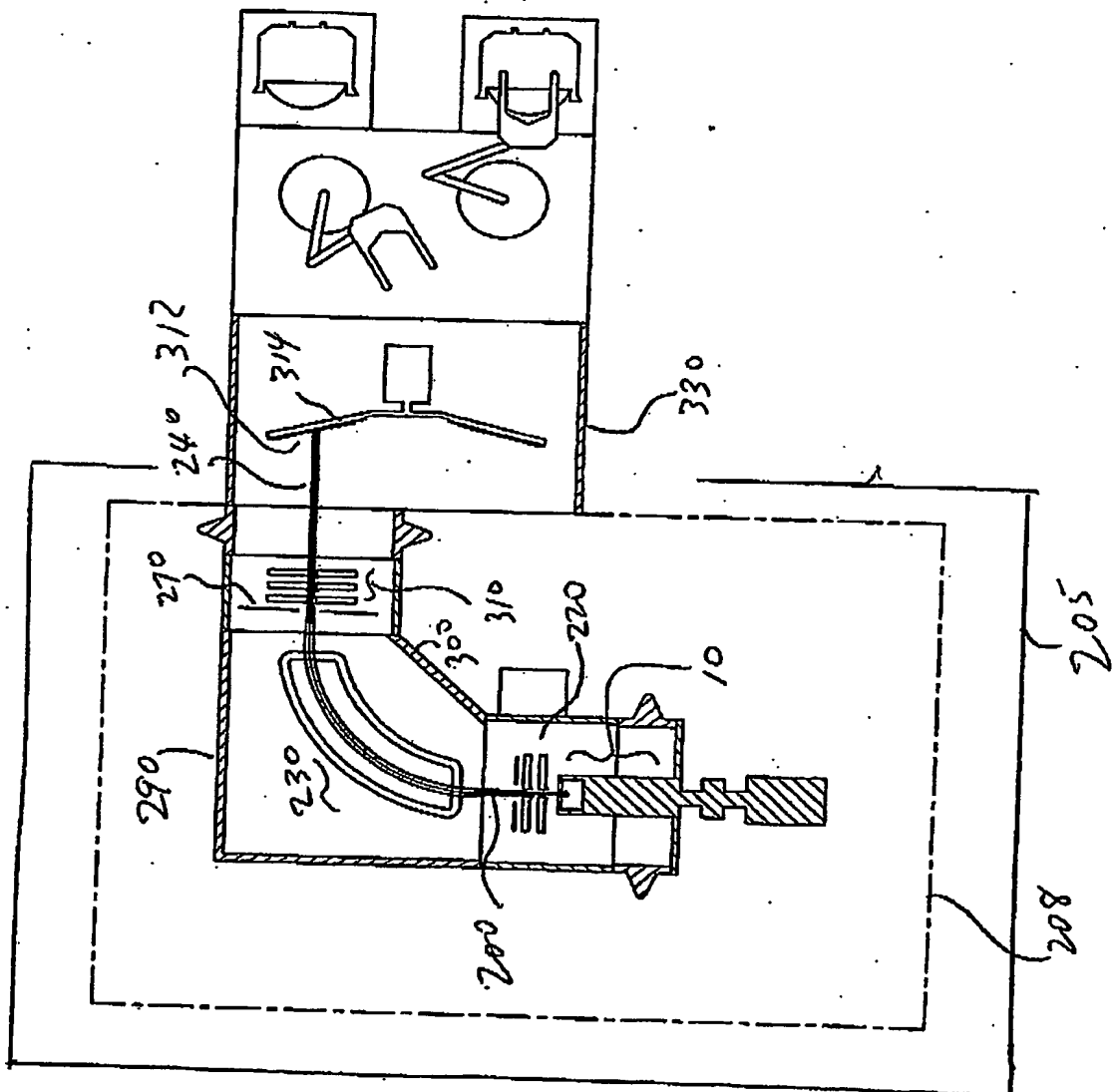


Fig. 1(c):

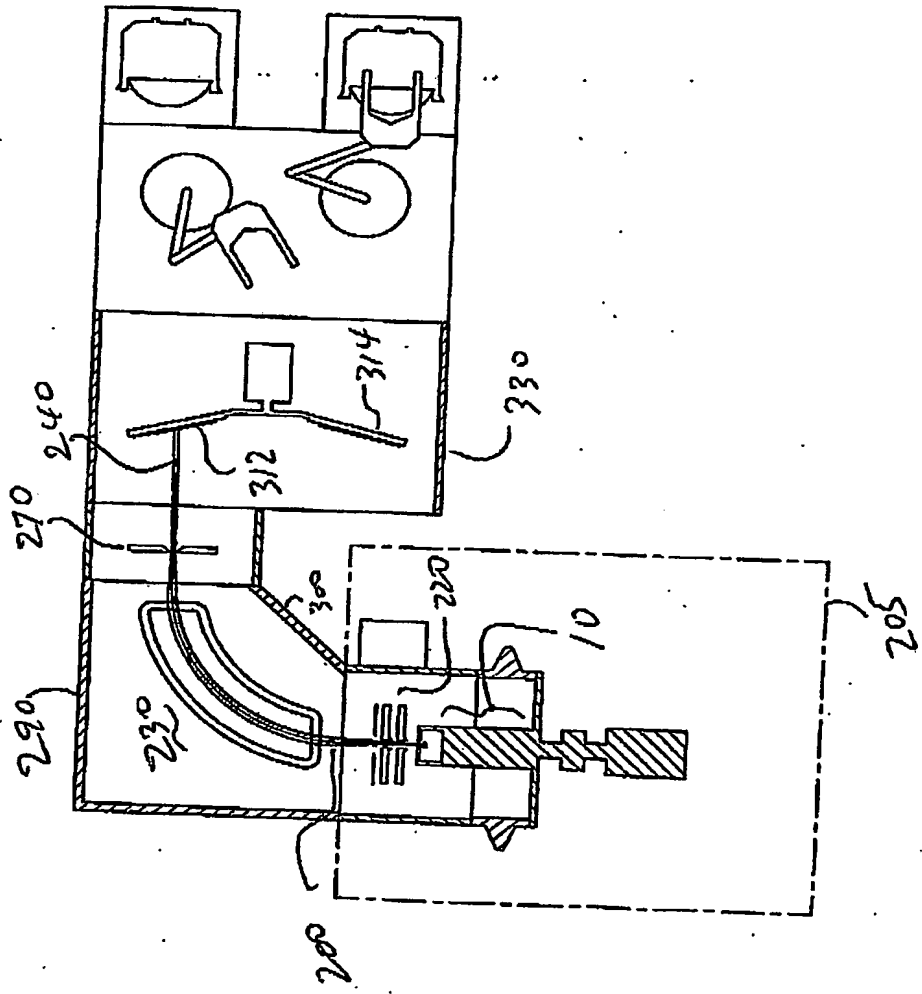


Fig. 1 (d)

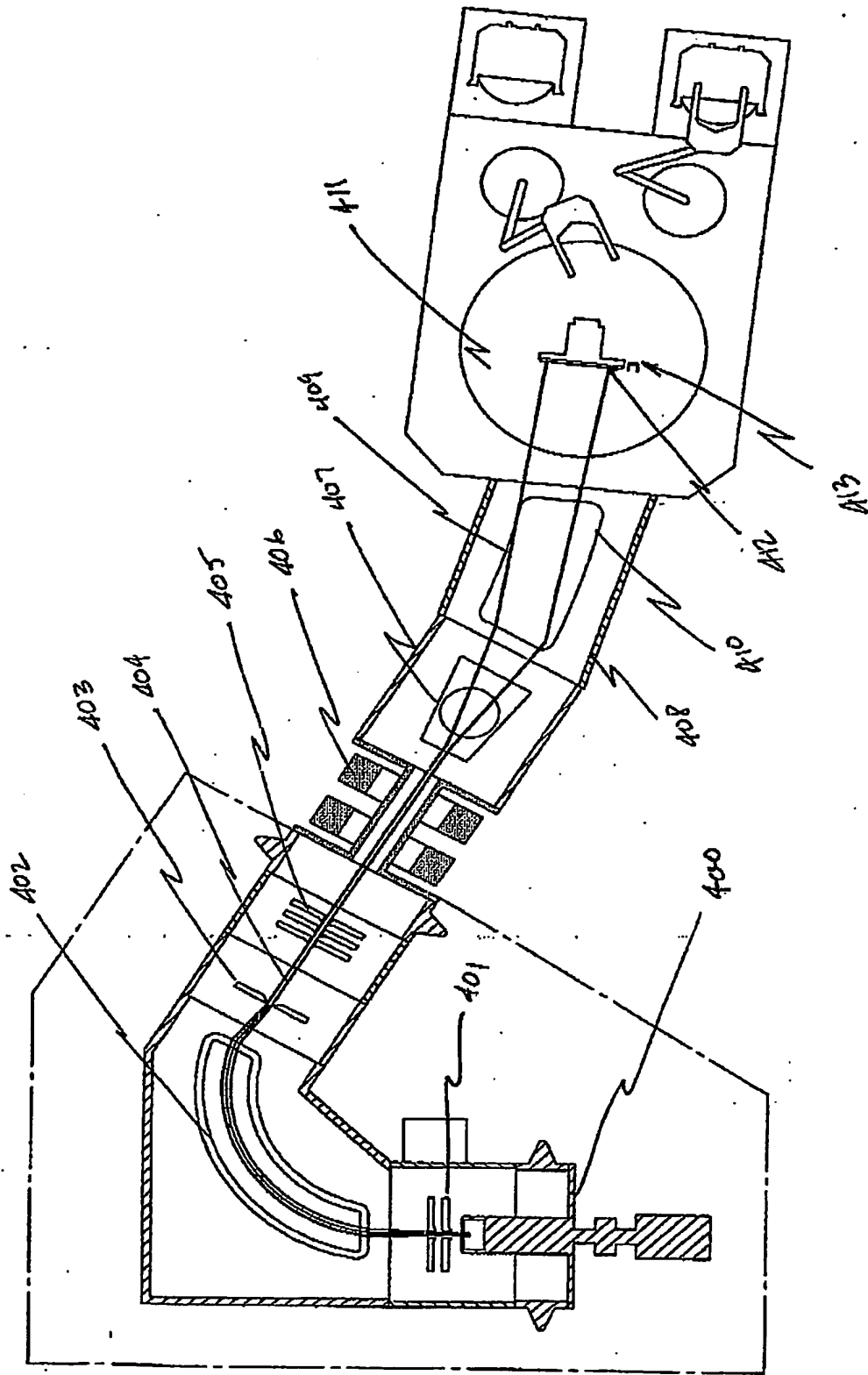


Fig. 1(e)

Space Charge-Limited Extraction of Boron Monomer Ions, for a Diode Gap of
1.27 cm, Calculated from Child-Langmuir

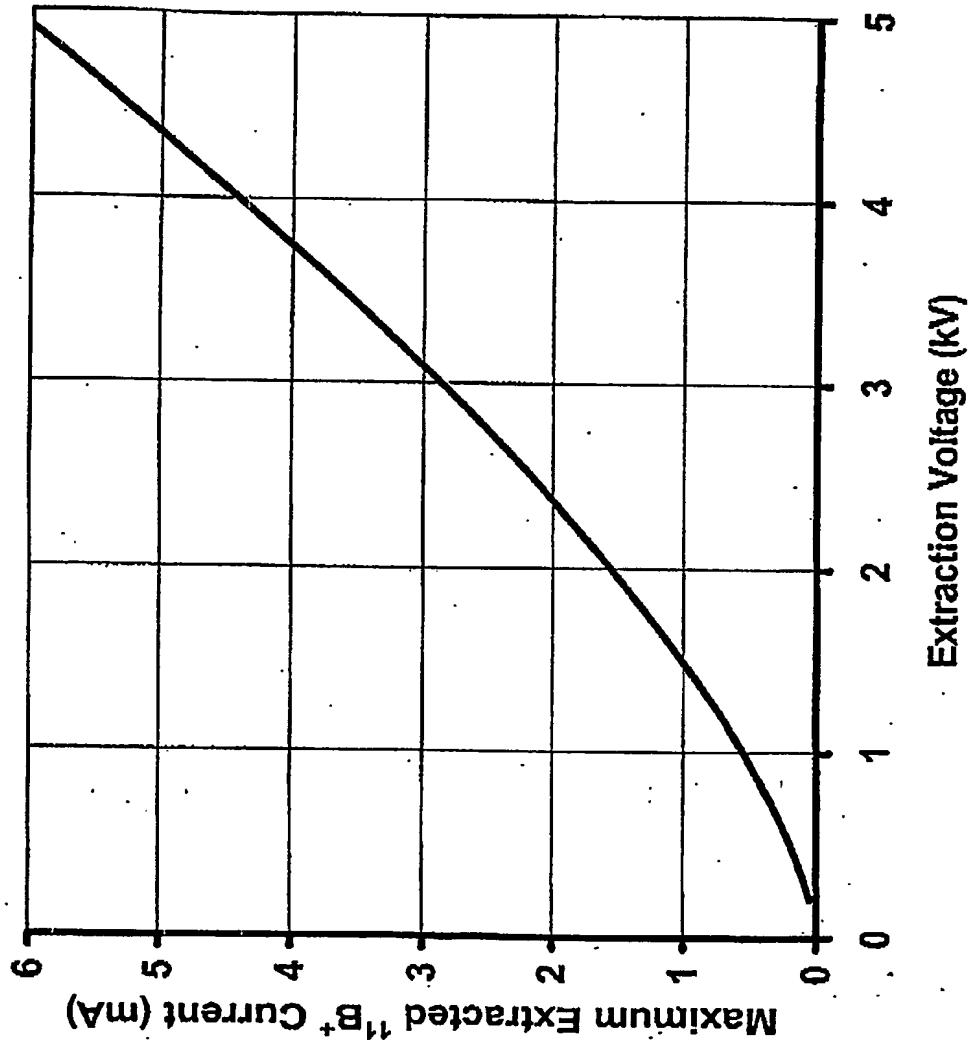


Fig. 2.

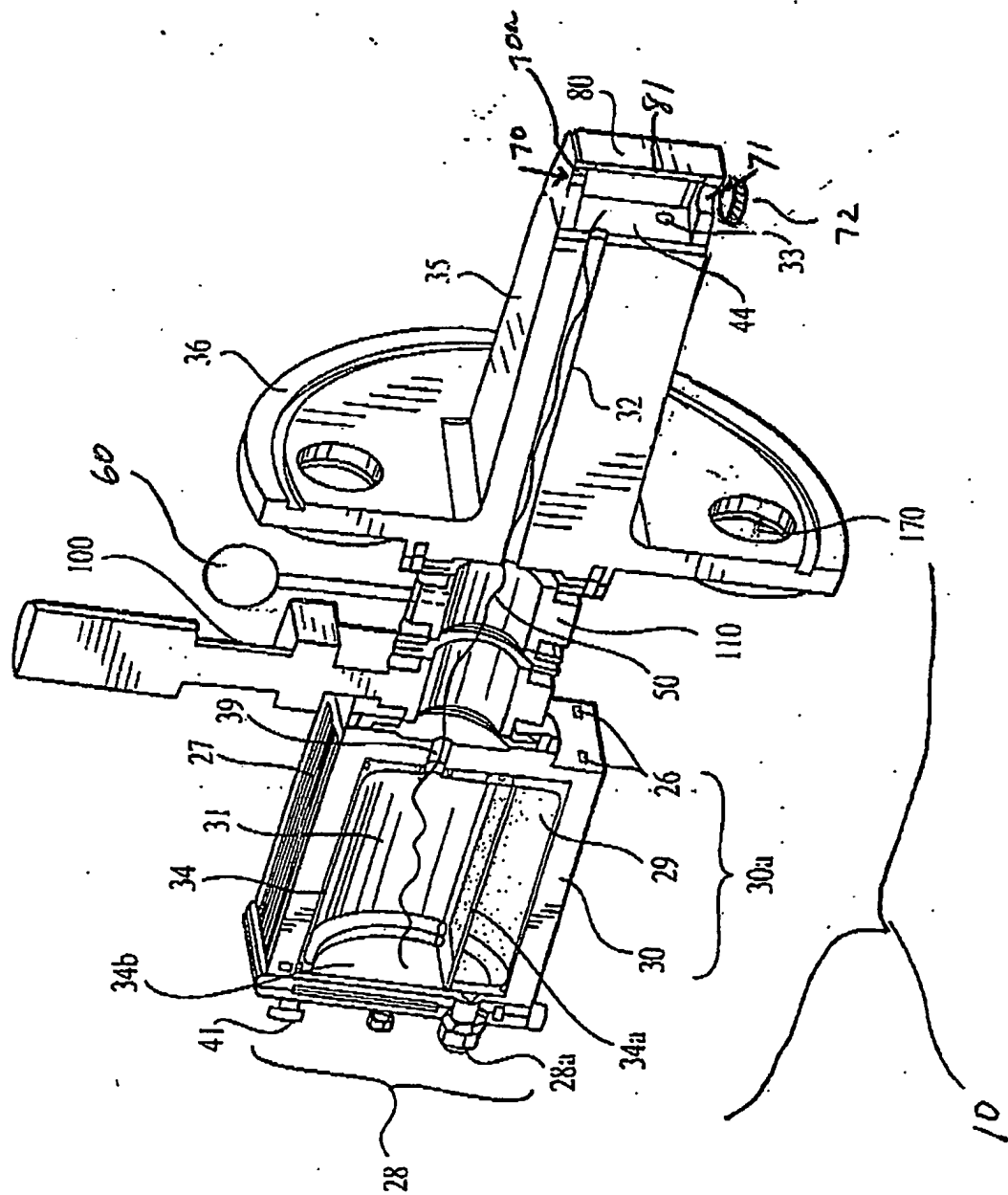


FIG. 3

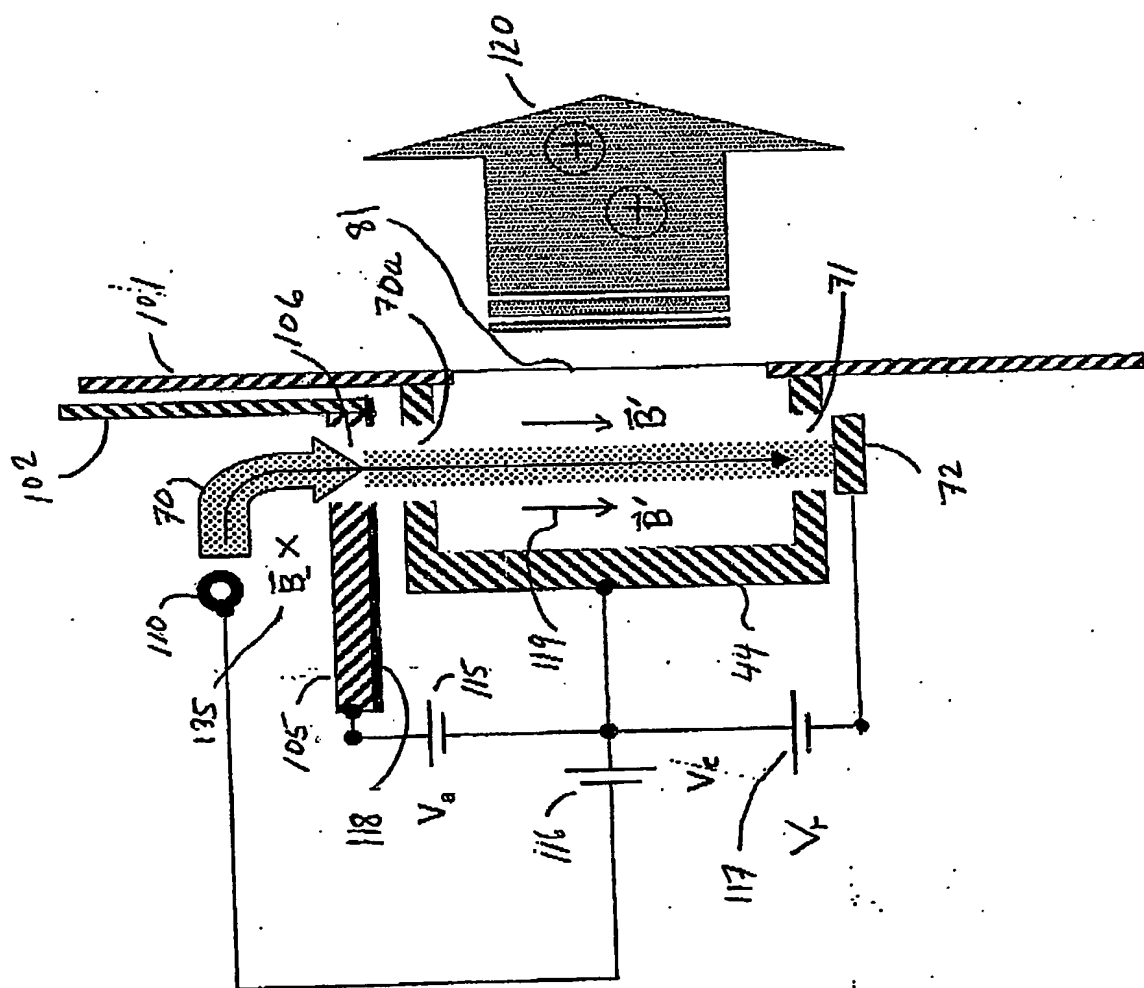
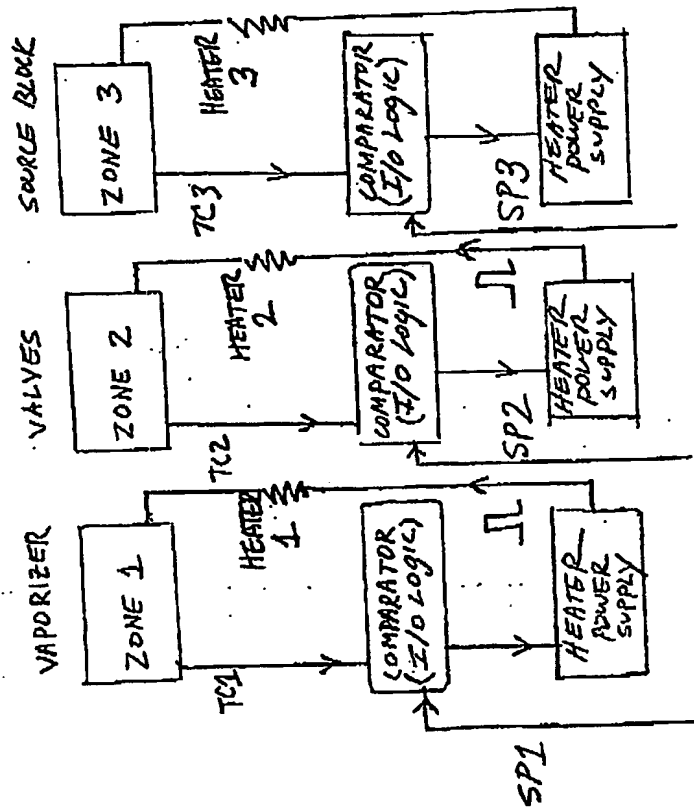


Fig. 4



3-Zone Temperature
Control System
FIG 6

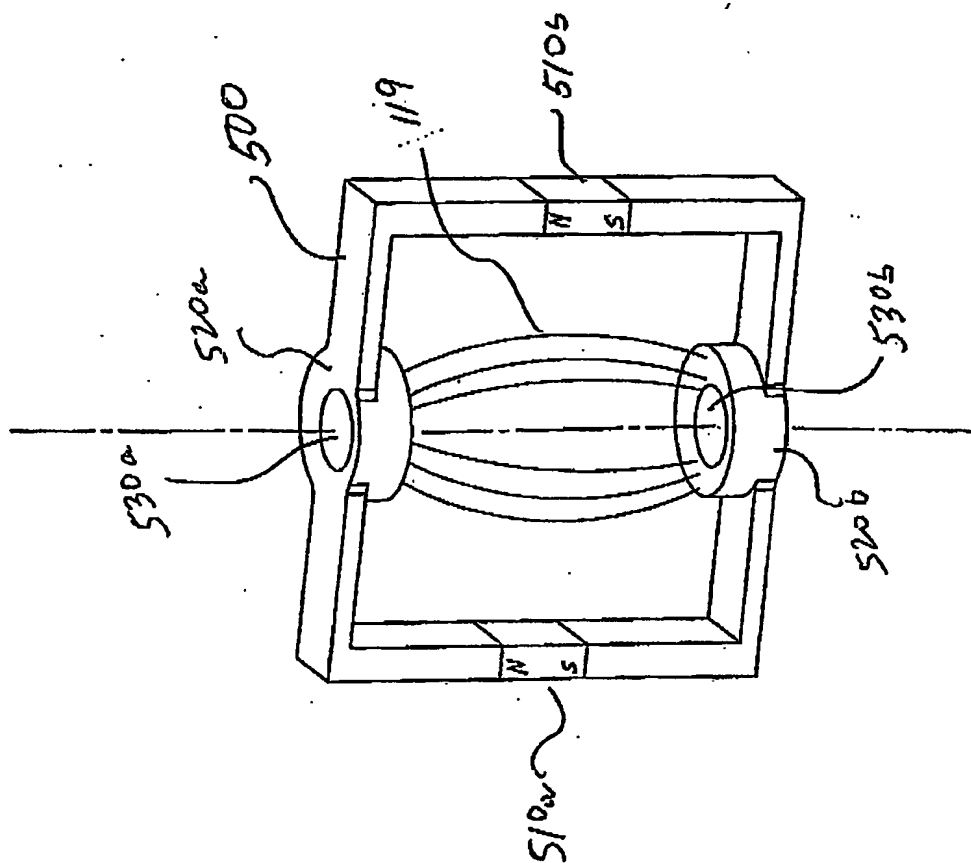


Fig. 7

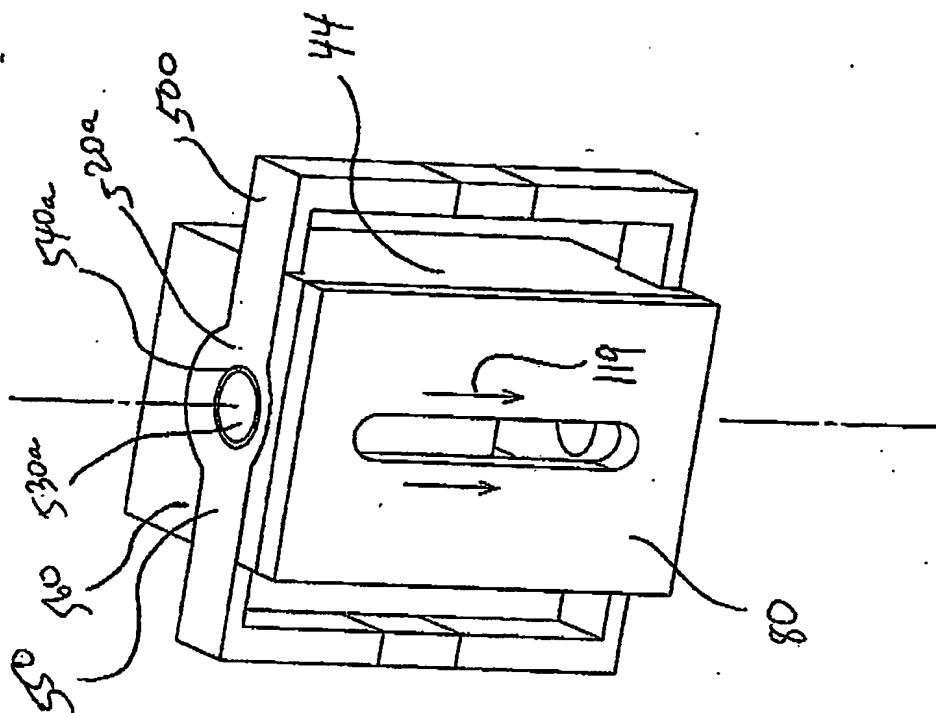
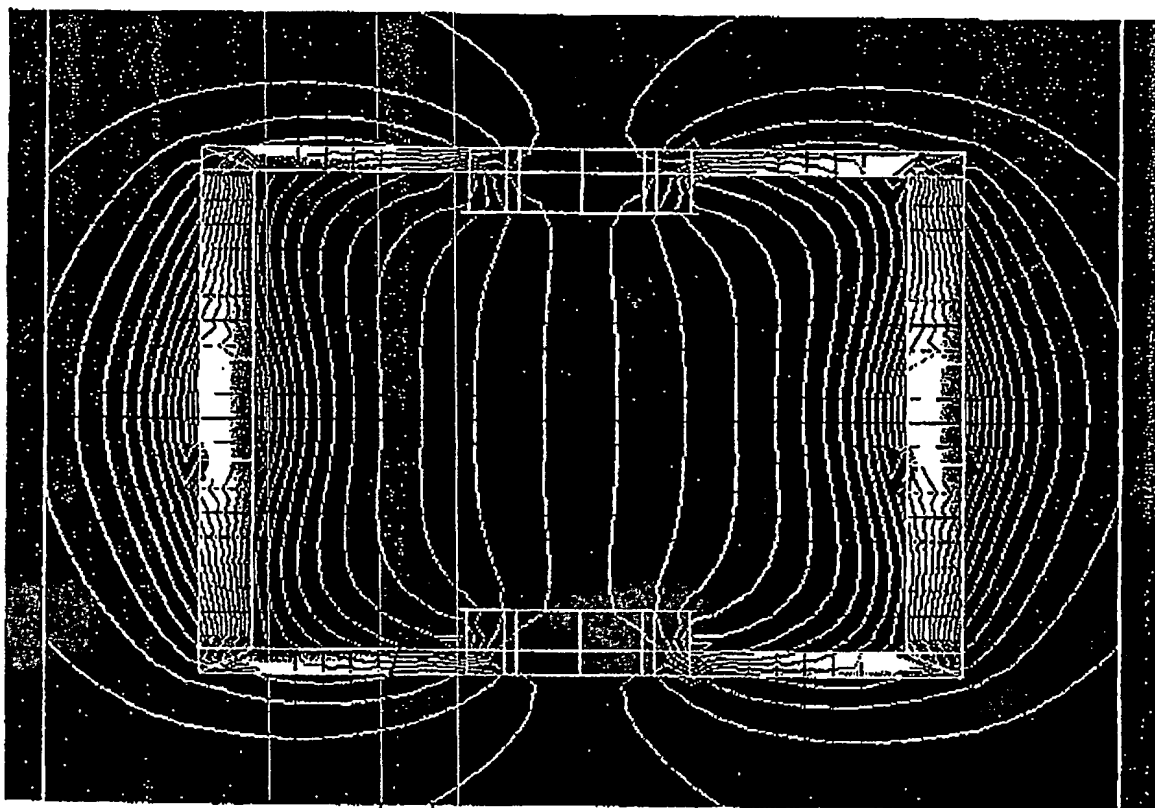


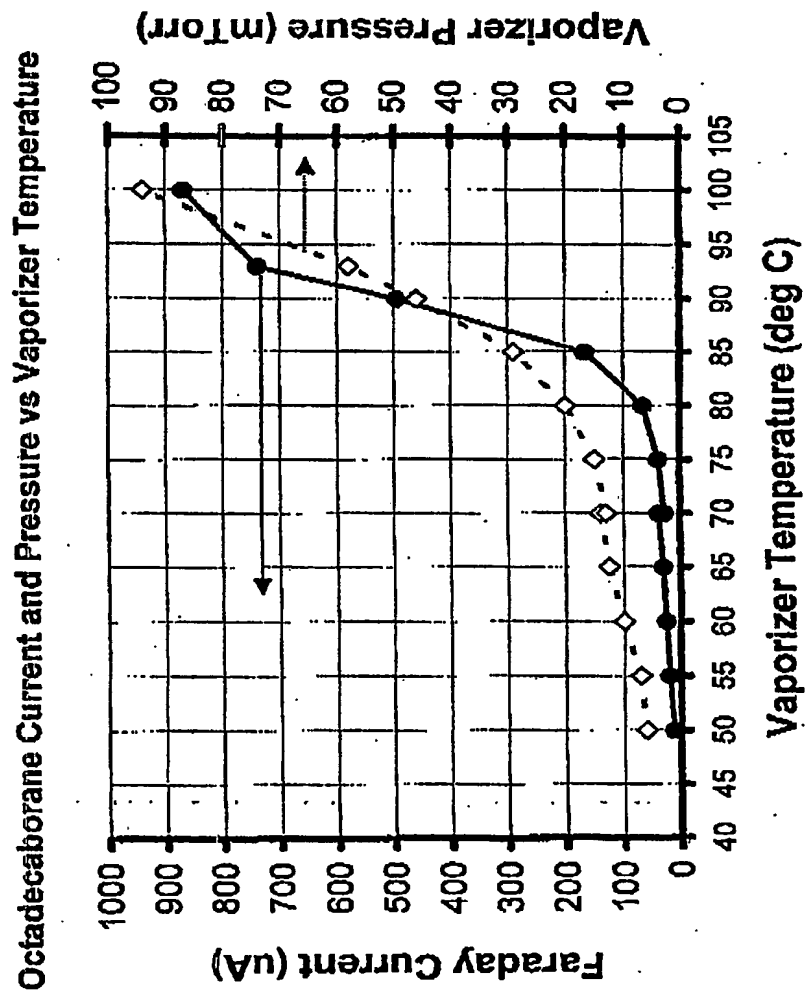
Fig 7(a)

(9) L 64



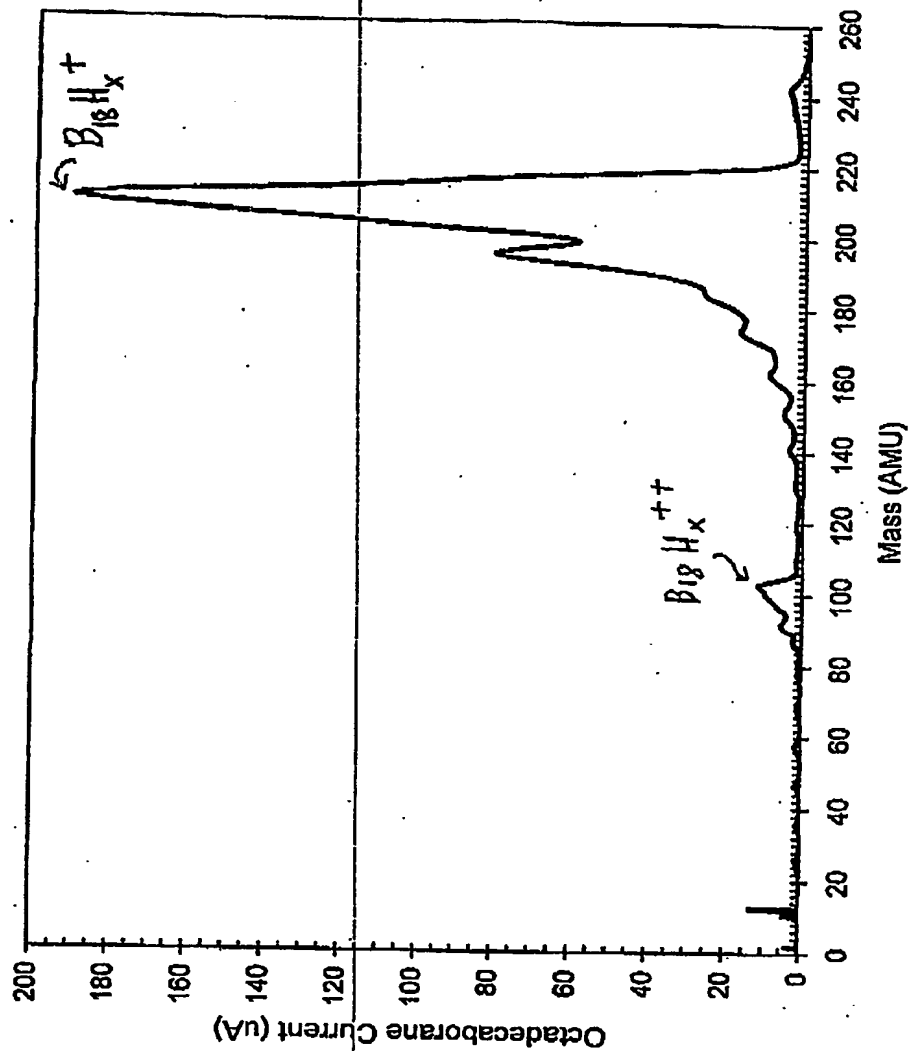
511

Fig. 8



MSR-10-5964-03

20keV Octadecaborane



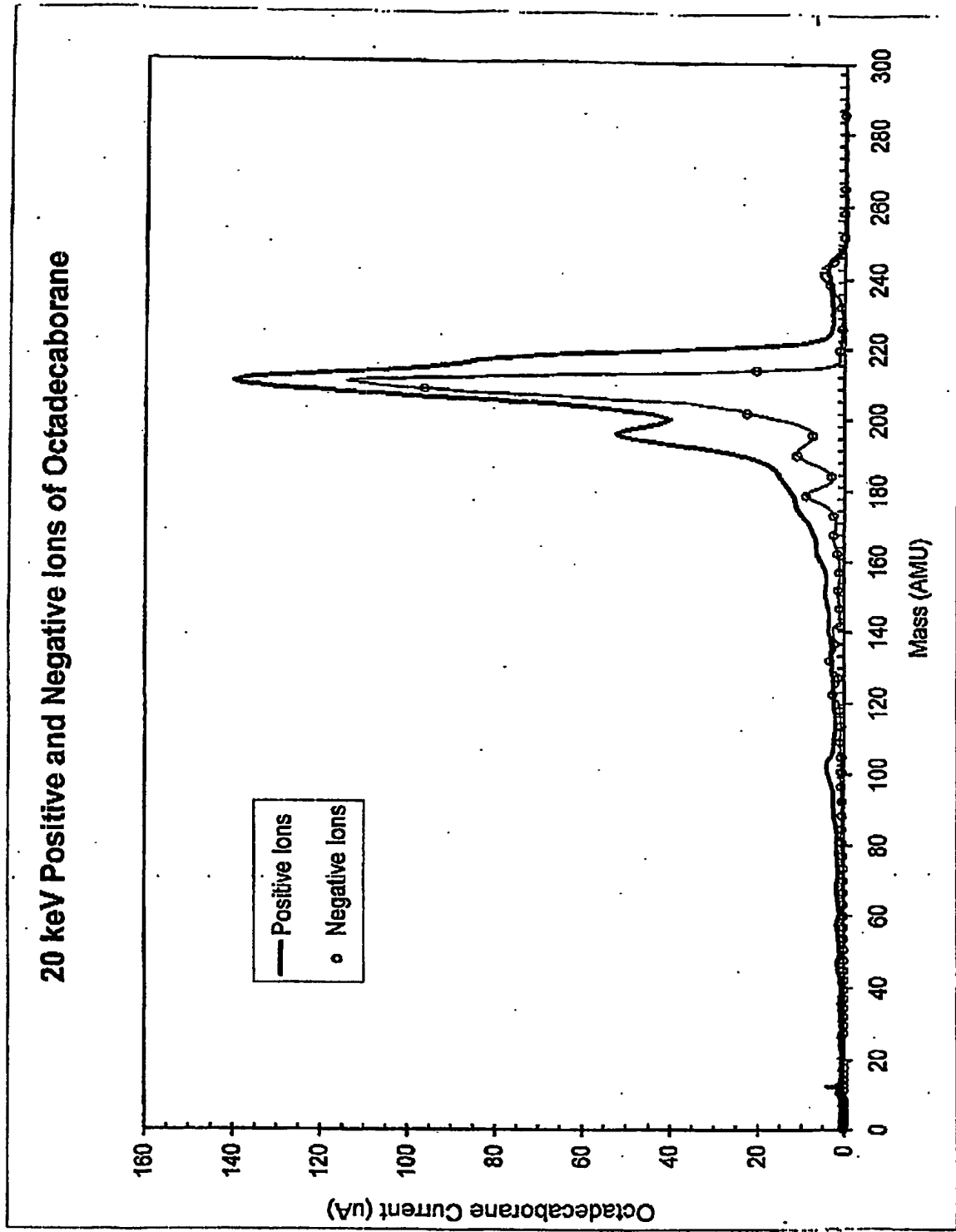


Fig. 10

20 keV Octadecaborane

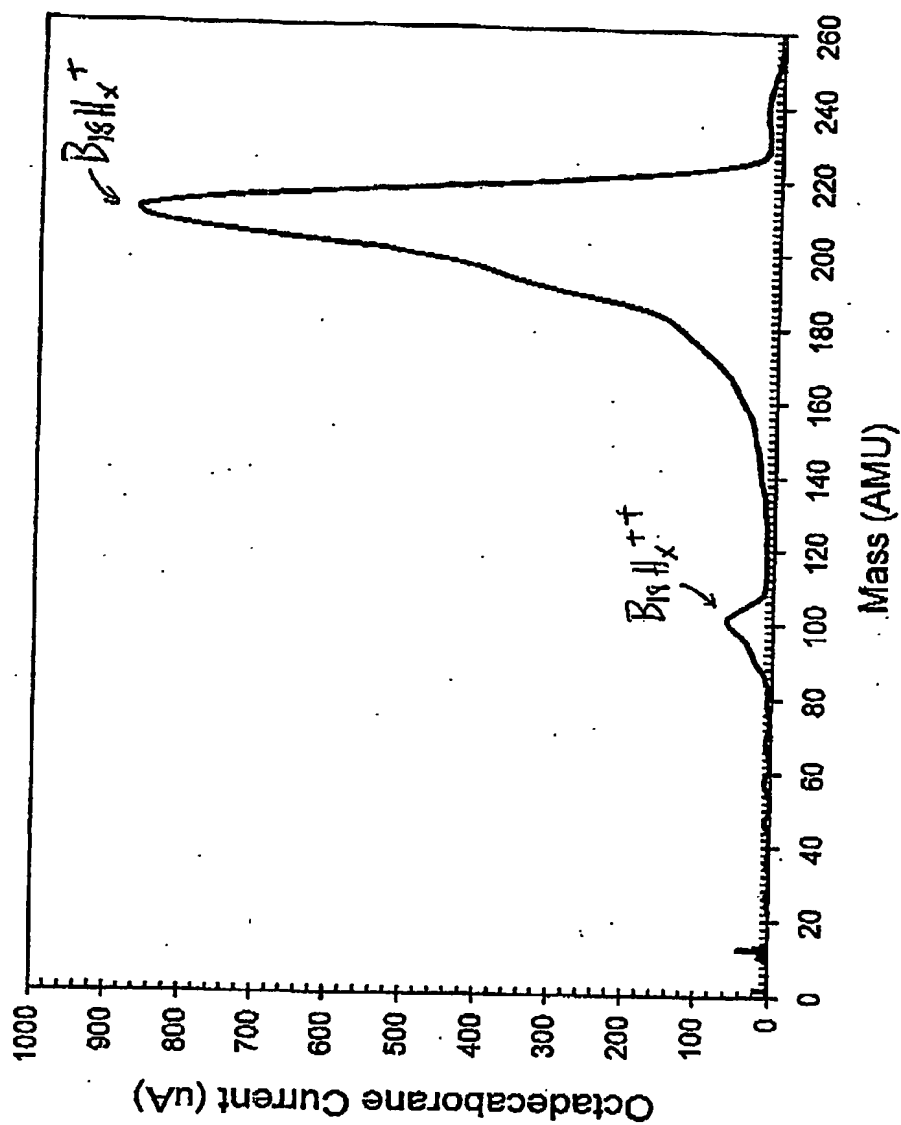


Fig. 11

Fig. 11

20 keV Octadecaborane

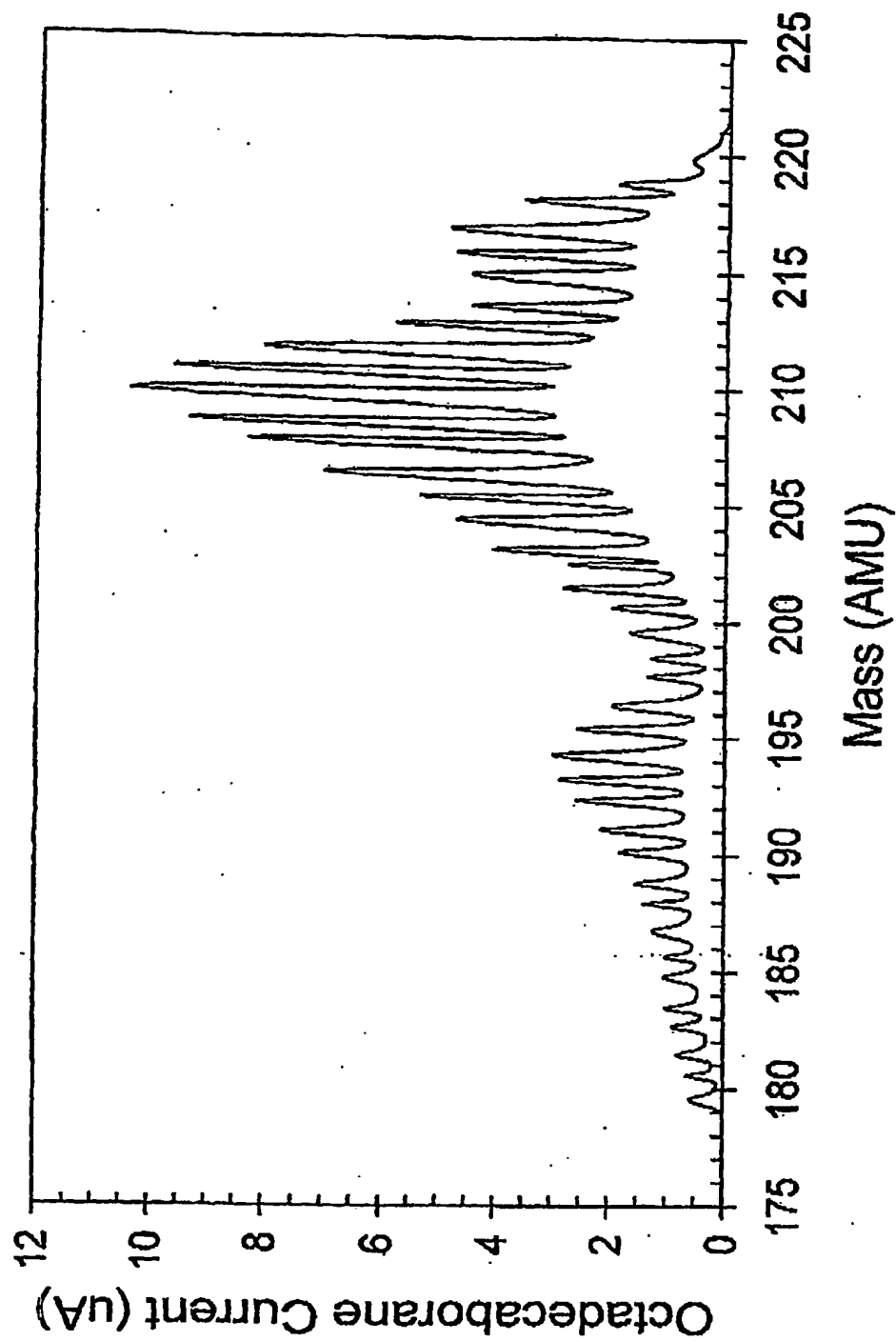


Fig. 11(a)

Octadecaborane Ion Current vs Energy

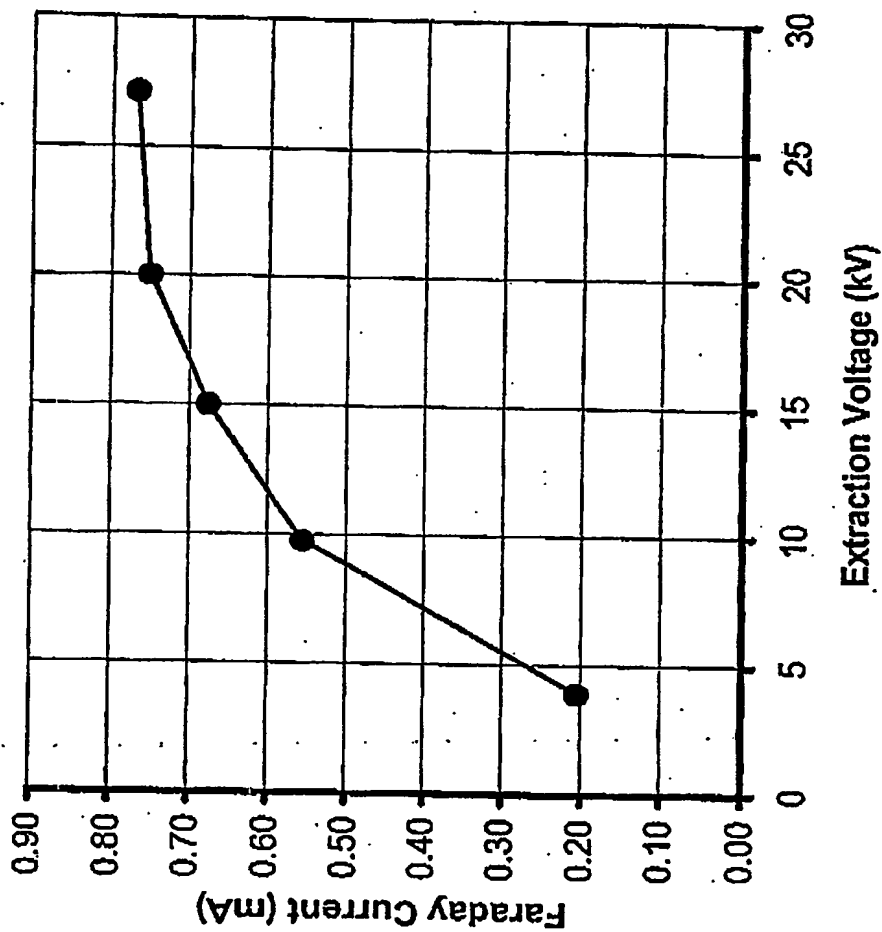


Fig. 12

Octadecaborane Boron Current vs Effective Implant Energy

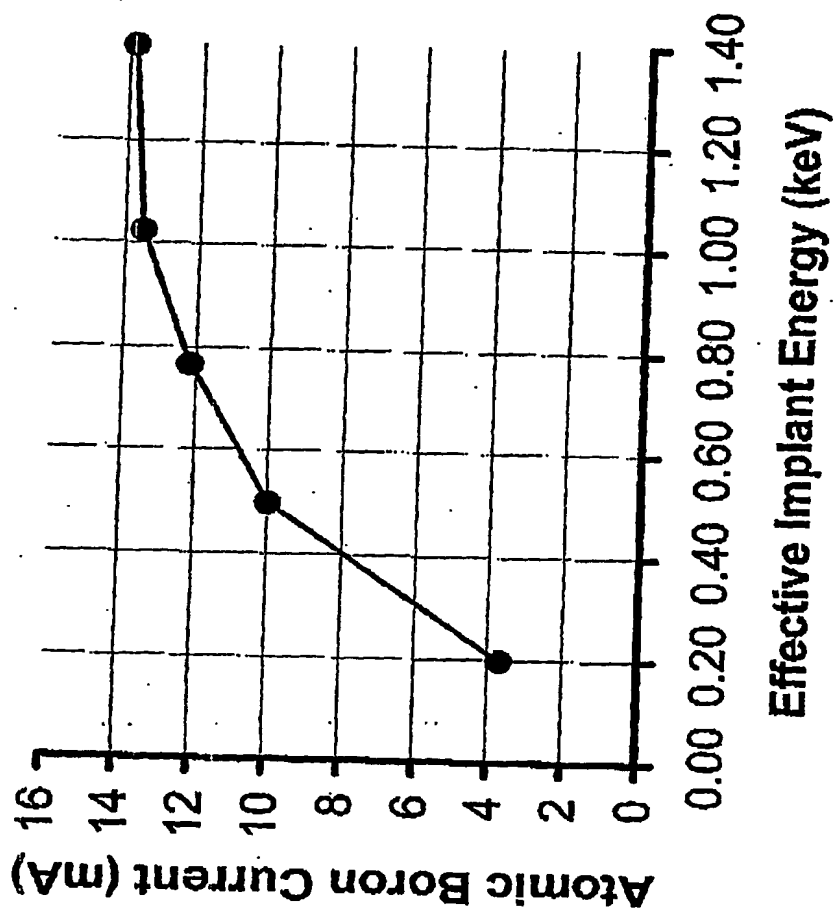
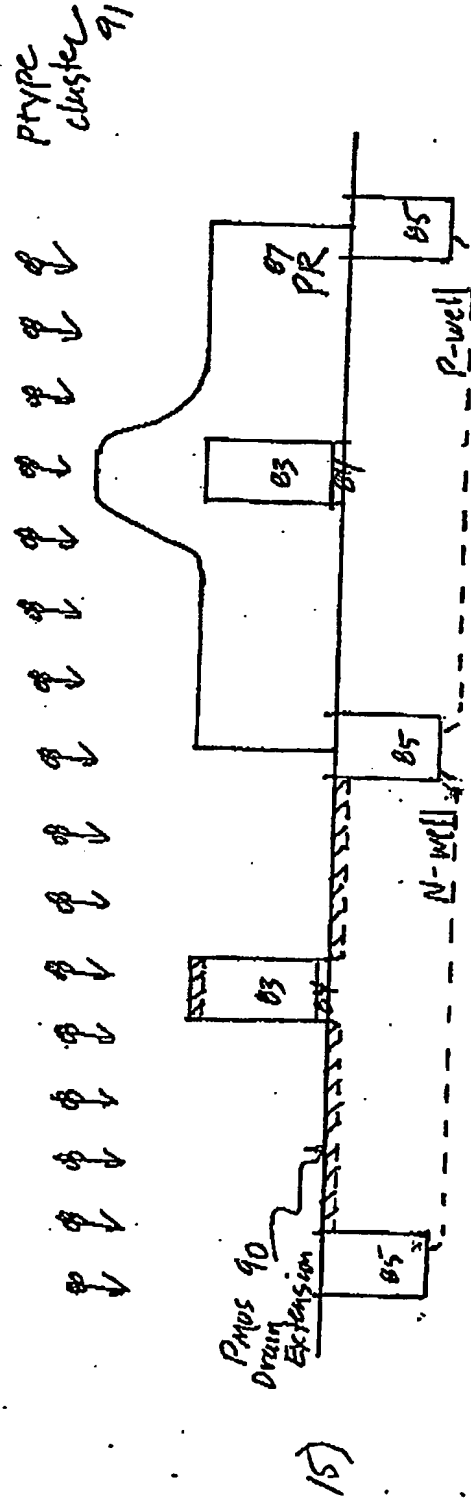
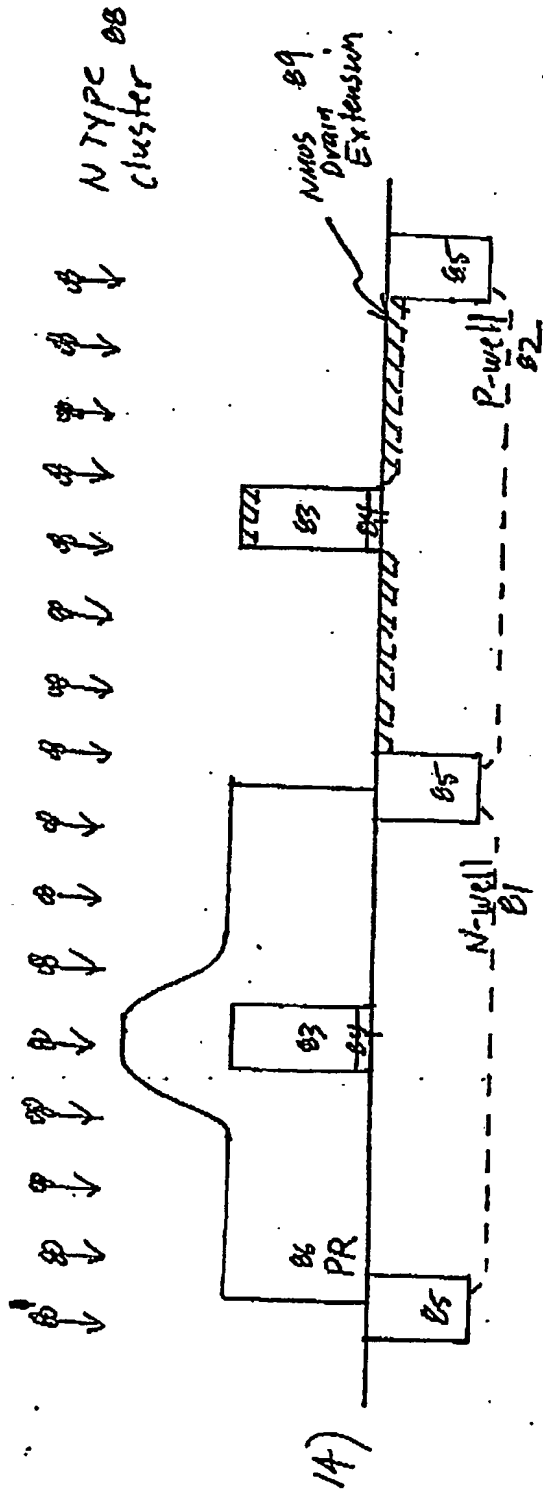


Fig. 13



P-channel transistor
PMOS

N-channel transistor
NMOS

Figs 14, 15: Example of CMOS fabrication sequence 14) NMOS Drain Extension
15) PMOS Drain Extension

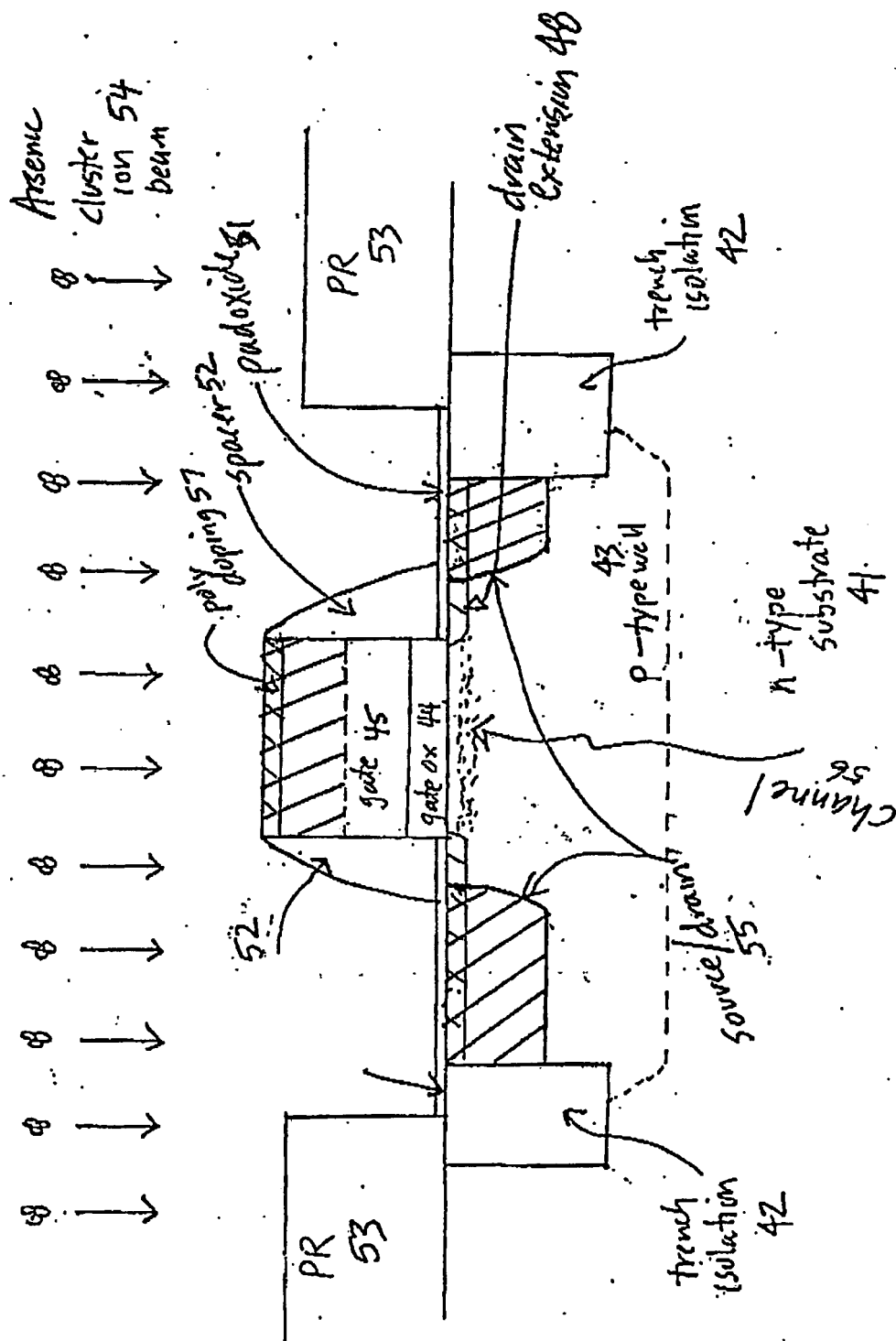


FIG. 17

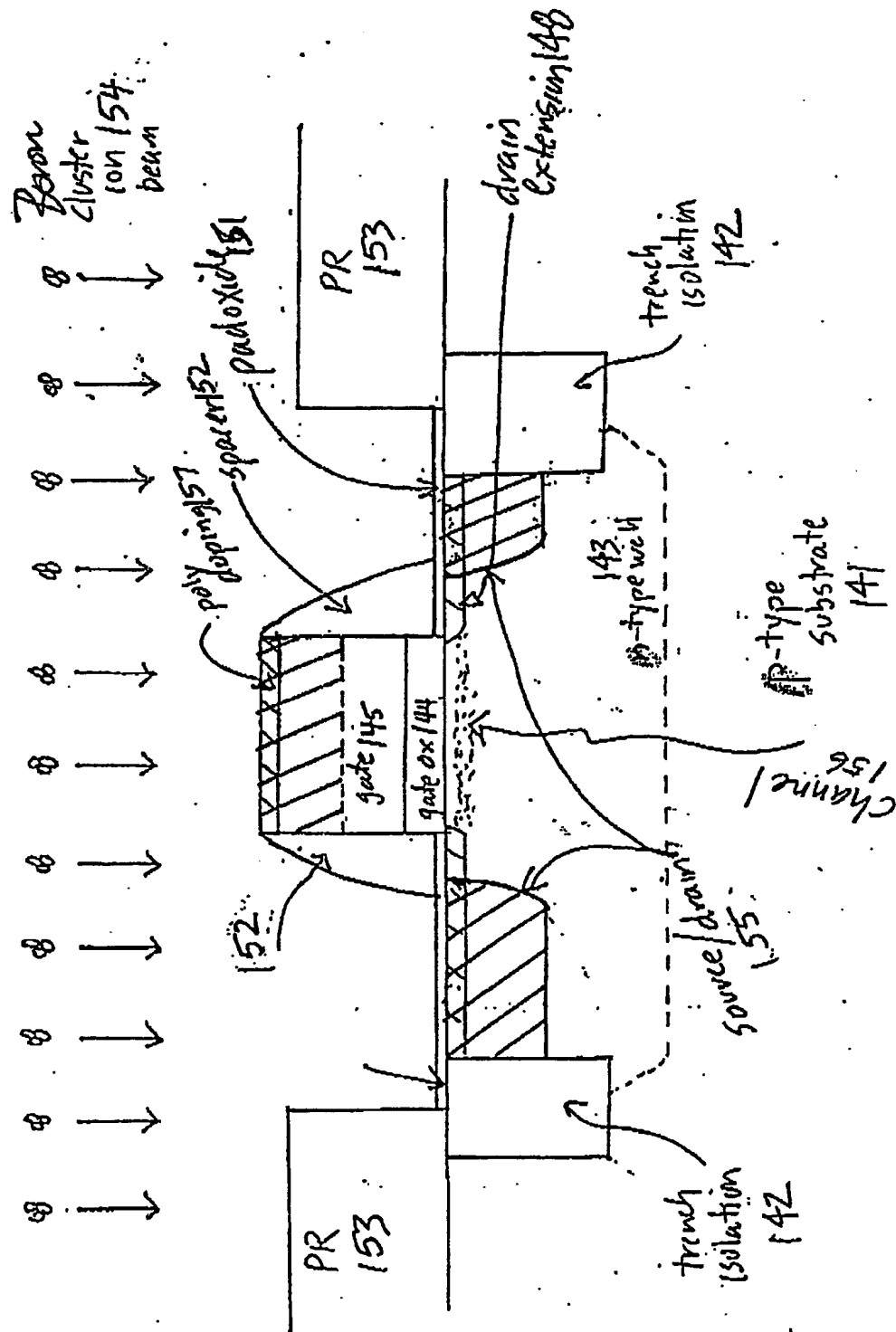


Fig. 19

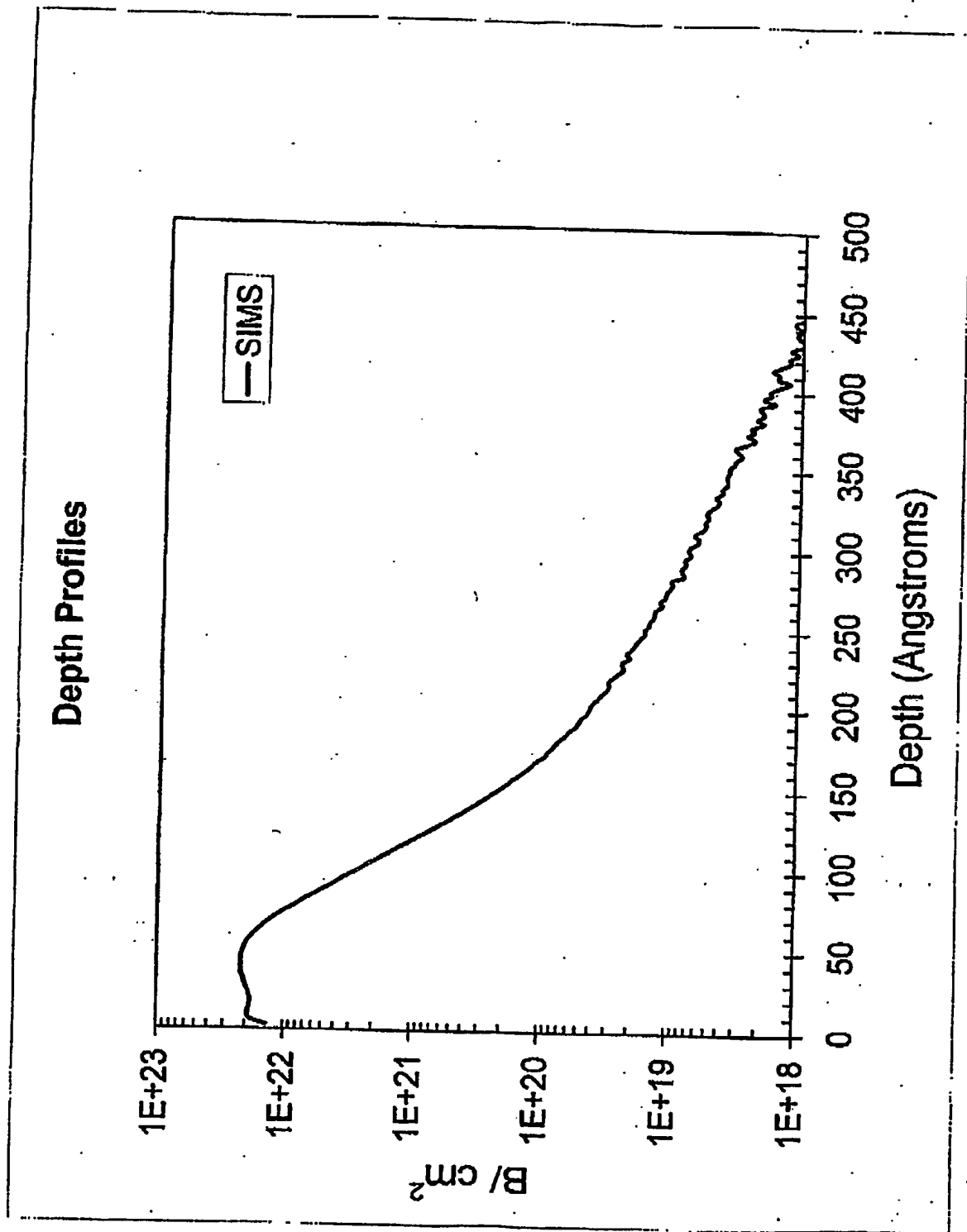


Fig. 20

**This Page is Inserted by IFW Indexing and Scanning
Operations and is not part of the Official Record**

BEST AVAILABLE IMAGES

Defective images within this document are accurate representations of the original documents submitted by the applicant.

Defects in the images include but are not limited to the items checked:

- ☐ BLACK BORDERS
- ☐ IMAGE CUT OFF AT TOP, BOTTOM, OR SIDES
- ☒ FADED TEXT OR DRAWING
- ☐ BLURRED OR ILLEGIBLE TEXT OR DRAWING
- ☐ SKEWED/SLANTED IMAGES
- ☐ COLOR OR BLACK AND WHITE PHOTOGRAPHS
- ☐ GRAY SCALE DOCUMENTS
- ☒ LINES OR MARKS ON ORIGINAL DOCUMENT
- ☐ REFERENCE(S) OR EXHIBIT(S) SUBMITTED ARE POOR QUALITY
- ☐ OTHER: _____

IMAGES ARE BEST AVAILABLE COPY.

As rescanning these documents will not correct the image problems checked, please do not report these problems to the IFW Image Problem Mailbox.